

Smart Analog Sensor Interface for Smoke Detection With Ambient Light Cancellation Reference Design



Description

This reference design provides a low BOM cost smoke detector design that passes UL217 9th edition sensitivity and fire room tests. Using a modulation-based photoelectric architecture, this reference design is able to achieve high rejection of ambient light for application in chambered or chamberless smoke detection. This design also has a high signal-to-noise ratio (SNR) for the entire signal chain that enables robust algorithms for reduced false alarms in smoke detector applications and particulate sensing in air-quality sensing applications. This design makes use of the low-power modes of the MSPM0L1306 microcontroller to achieve 10 years of battery life from a 9-V alkaline battery.

Resources

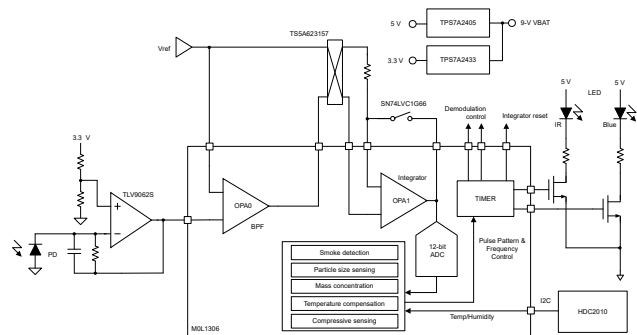
TIDA-010941	Design Folder
MSPM0L1306, TLV9062S	Product Folder
TPS7A2433, TPS7A2450	Product Folder
TS5A623157, SN74LVC1G66	Product Folder
HDC2010	Product Folder

Features

- Modulation-based sensing signal chain with ambient light rejection
- Advanced compressive sensing technique for low-power operation
- Dual-wavelength, dual-angle optical design for reduced false alarm smoke detection and particulate air-quality sensing
- Signal chain SNR of 77 dB (300 pulses)
- Total current consumption of 5.8 μ A (16 pulses, 0.1-Hz output data rate (ODR)) for 10+ years battery life with 9-V alkaline battery
- Passes UL217 9th edition sensitivity and fire room tests

Applications

- [Smoke and heat detector](#)
- [Wireless environmental sensor](#)
- [Air purifier and humidifier](#)
- [Air conditioner indoor unit](#)



1 System Description

Recent changes to the UL217 standard for residential smoke alarms (eighth and ninth editions) have been made to improve the performance of smoke alarms; first to keep up with modern construction techniques and materials, such as lighter more flammable materials in open floor plans that lead to hotter and faster burning fires which reduce the egress time needed for escape, and secondly to cover smoldering polyurethane fires which are not reliably detected with today's alarms. Additionally, to further improve reliability, the ability to distinguish between real sources of fire and nuisance sources, for example, from cooking, steam from a shower, and so on, is required. Smoke from these nuisance sources tend to contain particle sizes much smaller than those found in sources from real fires. However, flaming polyurethane is an exception, where the particle sizes in this type of smoke consists of sizes in the upper range as those found in nuisance sources. Currently available, single wavelength photoelectric detectors using simple threshold-based detection algorithms, do not have the capability to distinguish between certain types of smoke particles (for example, flaming polyurethane) and nuisance sources. The UL268 standard covering commercial smoke detectors has similar updated requirements for smoke sensing performance. The TIDA-010941 demonstrates a multi-wavelength, multi-angle design capable of passing the new UL217 9th edition sensitivity and fire room testing requirements.

This reference design uses a modulation-based signal chain to overcome several shortcomings of a traditional DC-based architecture. The two main advantages of this approach are the improvement of ambient light rejection and improved signal-to-noise ratio (SNR) for the signal chain. Low cost is paramount for smoke detector applications. The improved ambient light rejection of this design enables the potential to implement a chamberless smoke detector design. Removing the optical chamber in a photoelectric detector represents a significant savings in terms of both BOM and assembly costs. However, despite the benefits of not having a chamber, significant environmental challenges exist, such as rejection of disturbances due to insects or collection of dust in the optical path over time. Using a multi-wavelength architecture, in this case Blue and Infrared (IR), allows for an increased signal response from smaller particle sizes typically found in nuisance sources, thereby, increasing the effective particle size detection range of the signal chain. The multi-angle aspect of this design consists of measuring the light scattering response at different scattering angles such as a typical forward scatter angle and a back scatter angle. This allows the estimation of particle size by taking the ratio of the measurements from the two angles. These two techniques; multi-wavelength and multi-angle, together, allow for a robust multiple-criteria approach for distinguishing between real sources of smoke and nuisance sources.

The improved SNR for the signal chain in this design not only enables the implementation of robust algorithms for reduced false alarms in smoke detection, but also enables the ability to sense particulates in air quality sensing application. Very accurate particle size estimates as well as mass concentration measurements are possible with this reference design. The implication is that this design opens the door for a smoke detector capable of not only meeting the latest standards for smoke detection but also sensing indoor air quality using the same optical design.

Lastly, low power is a key concern for smoke alarms that are battery operated since changing batteries frequently is inconvenient and quite challenging in certain installations for the consumer. The TIDA-010941 is capable of providing 10 years of battery life from a single 9-V alkaline battery to make sure smoke detection remains operable for as long a possible.

1.1 Key System Specifications

DESCRIPTION	PARAMETER	SPECIFICATIONS	NOTES
Module	Input Power Source	5.5 V to 18 V (9-V Battery) 5 V ± 5% (ext.)	9-V alkaline input or external input header
	Ambient Temperature Range	0°C to 50°C	
	Estimated Battery Life	10.2 years	650 mAh, 20% Derating factor, no alarms
Receiver Only	RX Signal Chain Gain	0.137 nA/LSB	$f_{\text{mod}} = 115 \text{ kHz}$
	ADC Saturation Level	280 nA	
	Ambient current headroom	15 μA	ADC Saturation
	Ambient Light Rejection	57 dB	at 120 Hz
	Total input referred noise	18 pA _{RMS}	300 pulses
	SNR	84 dB	300 pulses
Signal Chain	SNR (90% full scale)	77 dB	300 pulses
	Particle Size	300 nm – 10 μm	± 0.2 μm error
	Mass Concentration	> 1 mg/m ³	± 20% error
	Total Current Consumption at 9 V		4.5 μA
		5.8 μA	16 pulses; 0.1-Hz ODR

2 System Overview

2.1 Block Diagram

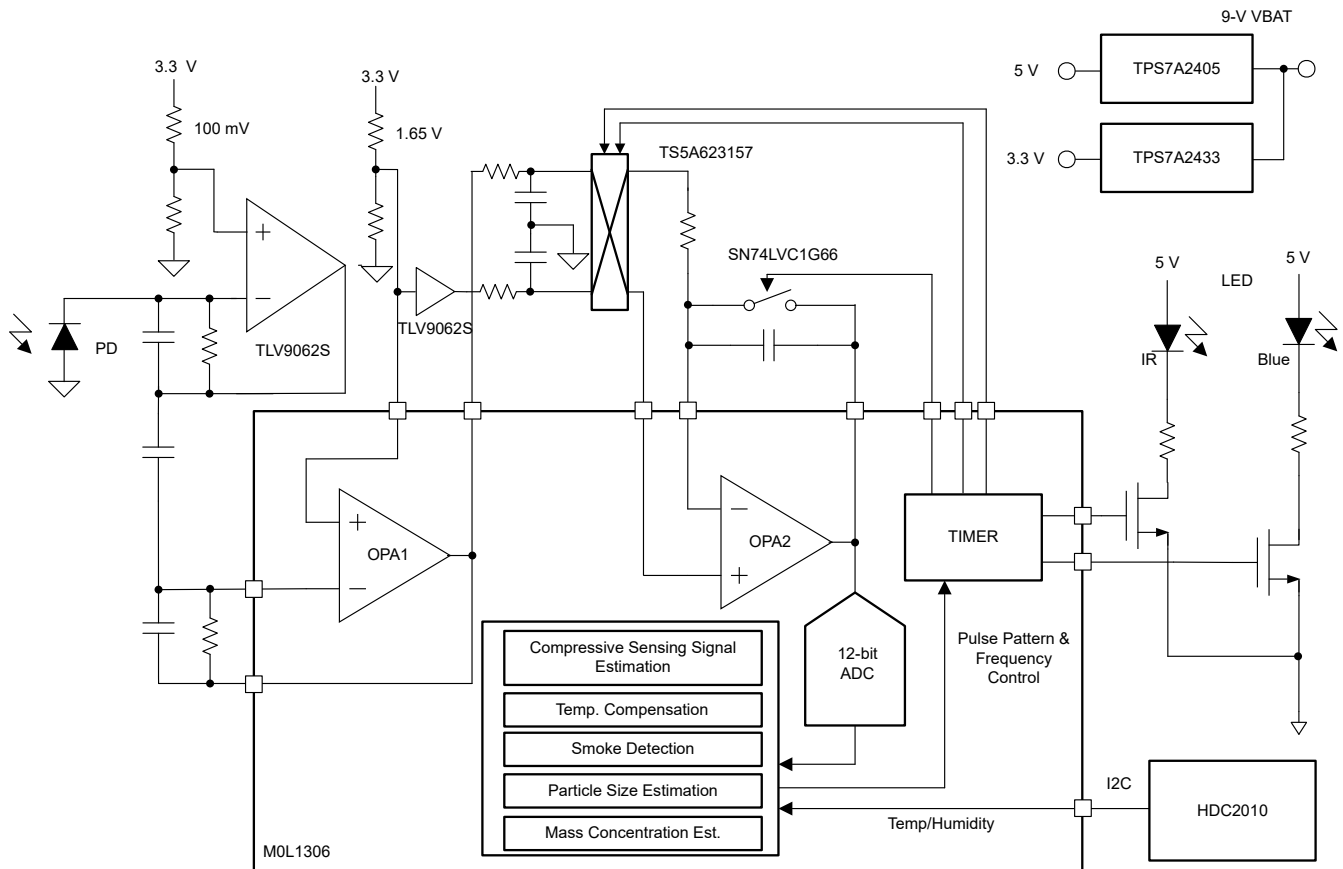


Figure 2-1. TIDA-010941 Block Diagram

2.2 Design Considerations

The TIDA-010941 provides a robust smoke detection design that is powered from a 9-V alkaline battery that is typically found in use as the backup battery in smoke alarms installed in homes. This design can also be powered from an external 5-V power source.

This design also allows for optimizations in both hardware and firmware for customizations to be made for meeting different product specifications. A GUI is provided for data capture and post-processing in addition to all necessary design and software files. CAD files for the 3D printed pieces used in this reference design are also made available.

This section outlines the theory and design considerations used to develop and design the TIDA-010941.

2.2.1 Photoelectric Smoke Detector Background – DC-Based Signal Chain

The optical smoke detector, also known as a photoelectric smoke detector, leverages the Mie light-scattering principle to detect the smoke particles rapidly and accurately. Figure 2-2 shows a simplified example of how this detector works. The light-emitting-diode (LED) is pulsed periodically to transmit the light across the detection zone. If there are no smoke particles, minimal light reaches the photosensitive element (photodiode in this case) and hence no smoke alarm is triggered. When there are smoke particles, the pulsed-LED light is scattered to the photodiode (PD) and is translated to an electrical signal with sophisticated front-end circuitry. Once the signal surpasses a certain threshold, the smoke alarm is triggered.

The detection happens in the optical chamber with both optical elements being inside the chamber. The optical chamber serves two goals: (1) the chamber blocks external light from the environment as well as undesired

objects such as insects to avoid any false alarm, but allows smoke particles to successfully enter the detection zone, (2) the internal mechanical and material design makes sure that negligible light reaches the photodiode when there is no smoke.

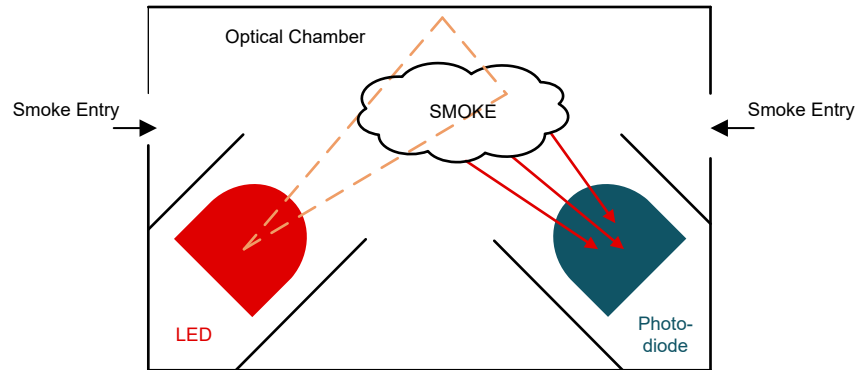


Figure 2-2. Detection Principle of Optical Smoke Detector

A conventional optical smoke detector uses a DC-based signal chain that samples the DC signal when the LED is on, but there are some drawbacks to this method. First, the ambient light from the environment acts as an interference signal, which is difficult to distinguish from the actual smoke signal as both are low-frequency signals. However, the optical chamber can be designed to block a majority of the ambient light. Secondly, the DC offset, flicker noise, and input bias current of the transimpedance amplifier (TIA) acts as an error signal for smoke sensing. As illustrated in Figure 2-3, these sources of error limit the signal-to-noise ratio (SNR) of the sensing signal chain.

The aforementioned drawbacks either diminish the performance and robustness or increase the design complexity (better optical chamber) and the cost (better electronics) of the smoke detector.

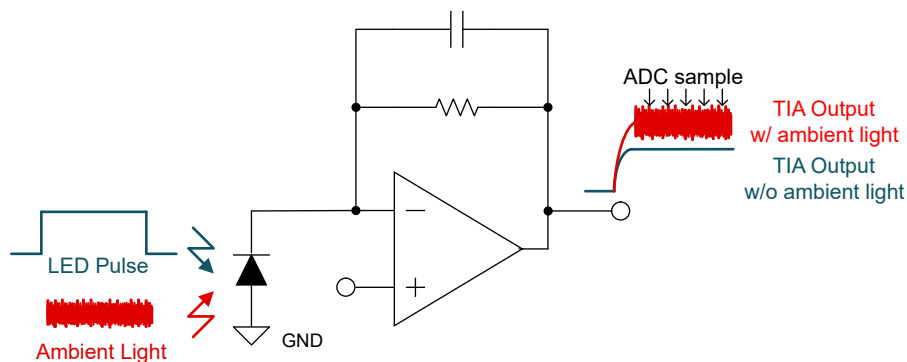


Figure 2-3. DC-Based Smoke Detection Signal Chain

2.2.2 Modulation-Based Smoke Detection Signal Chain

This design adopted a modulation-based smoke sensing signal chain to overcome the limitations of the DC-based signal chain. As shown in Figure 2-4, the smoke signal is modulated to frequency f_{mod} by sending a series of LED pulses at the frequency of f_{mod} . The frequency, f_{mod} , is selected to be far from the frequency of different types of ambient lights; for example, the LED and incandescent light interference located around 120 Hz along with harmonics of the 120-Hz fundamental frequency, and fluorescent light interference located around 44 kHz along with harmonics of the 44-kHz fundamental frequency. The modulated signal with ambient light interference is filtered by a bandpass filter with a center frequency located at f_{mod} . The interference is attenuated by the bandpass filter while the smoke signal is retained. The signal is then demodulated back into baseband while the low-frequency interference is modulated up to f_{mod} . With additional low-pass filtering, the interference is attenuated again, yielding an interference-free smoke signal around DC at the baseband. The demodulated signal is sampled by an Analog-to-Digital Converter (ADC) and stored for further post-processing. The modulation, demodulation, filtering and sampling is operated pulse by pulse. Better SNR can be achieved

by sending a higher number of pulses (stronger filtering, more averaging, and lower noise) at the cost of power consumption.

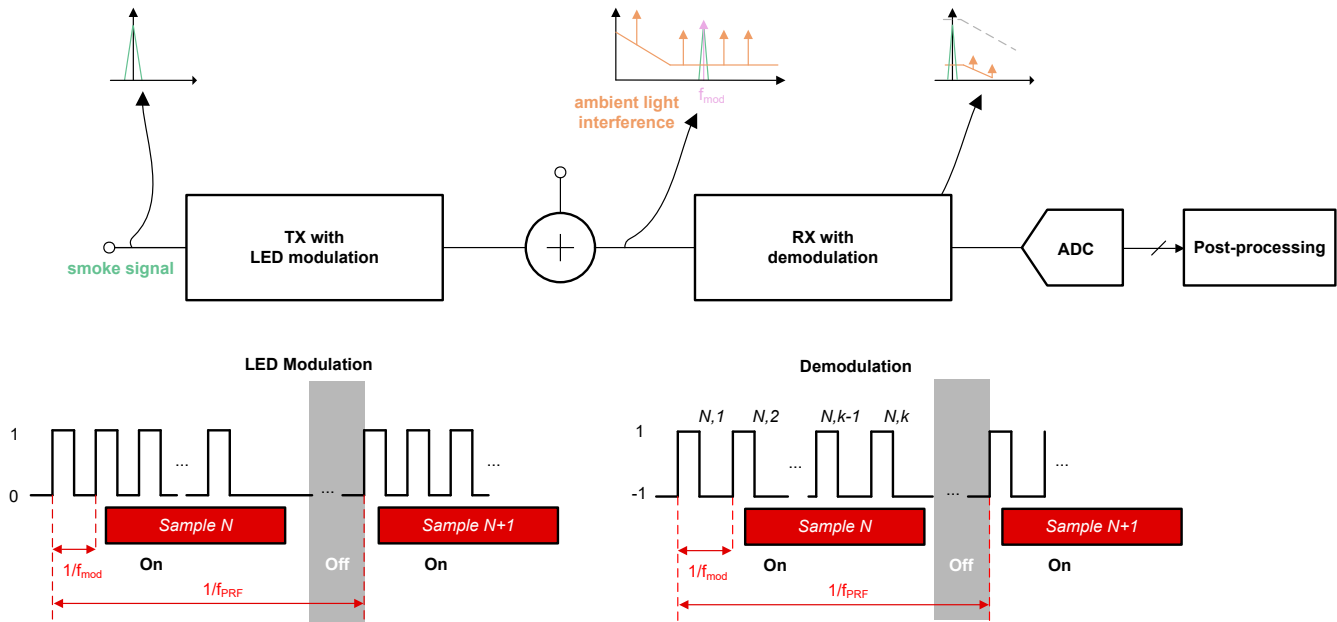


Figure 2-4. Modulation-Based Smoke Detector Signal Chain

2.2.3 Optical Sensing AFE Design

Optical power transfer ratio (PTR) is often adopted to represent the smoke intensity. PTR is given as:

$$PTR = \frac{I_{PD}/S_{\lambda}}{I_{LED} \times \eta_{LED}} \quad (1)$$

where

- I_{PD} is the photodiode current
- I_{LED} is the LED current
- S_{λ} is the photodiode responsivity at given wavelength
- η_{LED} is the LED efficiency

Typically, the smoke alarm trigger level ranges from 0.5 to 5 nW/mW across various fire types. This translates to a corresponding photocurrent of 5 to 100 nA if 100 mA is used for the LED drive current. The target noise performance in this design is less than 50 pA_{RMS} so that a 20-dB SNR can still be achieved even at the minimum current scenario for robust smoke alarm triggering. Therefore, a total signal chain gain of 5.8 MΩ is targeted in this design to achieve the target noise performance by minimizing the impact of ADC quantization noise.

Figure 2-5 shows the block diagram details that are adopted in the smoke detector signal chain. The overall signal chain gain can be calculated using Equation 2.

$$\frac{V_{out}}{I_{smoke}} = \frac{4}{\pi^2} G_{TIA} G_{BPF} G_{INT} \quad (2)$$

where

- I_{smoke} is the photocurrent induced by scattered light from smoke particles
- V_{out} is the integrator output voltage before ADC samples
- G_{TIA} is the Transimpedance Amplifier (TIA) gain
- G_{BPF} is the bandpass filter (BPF) gain
- G_{INT} is the integrator gain

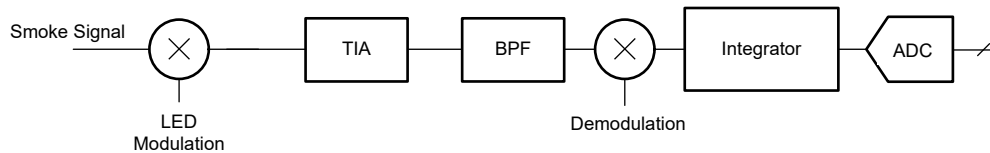


Figure 2-5. Modulation-Based Smoke Detector Signal Chain Block Diagram

2.2.3.1 TIA

The first stage of the AFE is a transimpedance gain stage consisting of a resistor-feedback TIA as shown in Figure 2-6. The goal of this stage is translating photocurrent to voltage for future stages as well as providing high gain. The op amp used in TIA is TLV9062S, which has a 10-MHz bandwidth, low broadband noise (10 nV/ $\sqrt{\text{Hz}}$) and rail-to-rail input and output (RRIO). The low noise and RRIO feature makes sure that the TIA has high dynamic range, and high bandwidth makes sure that there is compatibility with high modulation frequency and excellent stability even with large input photodiode capacitance. TLV9062S also has a shutdown option that keeps power low between smoke-sensing periods. The feedback resistor of the TIA is chosen as 249 k Ω to provide a transimpedance gain close to 249 k Ω . A 1.9-pF feedback capacitor is added to provide the TIA stability with an input photodiode capacitance up to 50 pF. The 3-dB bandwidth of TIA can be calculated as:

$$f_{3\text{dB}, \text{TIA}} = \frac{1}{2\pi R_{\text{TIA}} C_{\text{TIA}}} = 336.4 \text{ kHz} \quad (3)$$

The DC bias of the TIA is provided by a resistor divider as:

$$V_{\text{bias}, \text{TIA}} = \frac{R_{1\text{CM}, \text{TIA}}}{R_{0\text{CM}, \text{TIA}} + R_{1\text{CM}, \text{TIA}}} \times V_{\text{DD}33} = 98.9 \text{ mV} \quad (4)$$

The design choice of DC bias voltage (approximately 100 mV) is mainly determined by three aspects: (1) large DC current (approximately 12.8 μA) caused by ambient light can be tolerated without saturating the TIA, (2) sufficient op-amp bandwidth can still be provided when the input current pulse arrives compared to biasing at 0 V. Large resistor values (10 M Ω + 309 k Ω) limit the total current flow through the biasing branch (0.32 μA), allowing the branch to be always on with low power, (3) keeping the photodiode reverse-bias voltage low helps to reduce the leakage from the photodiode, which is especially important for high-temperature operation. Reverse-bias also reduces the photodiode capacitance detected by the amplifier.

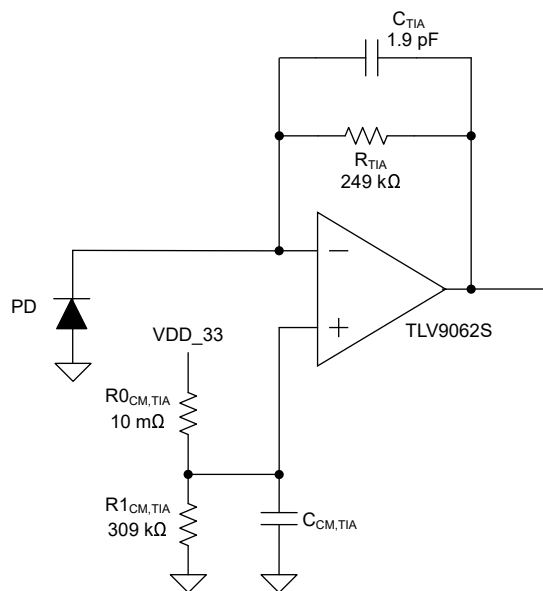


Figure 2-6. TIA Schematic

2.2.3.2 BPF

Figure 2-7 shows the schematic of the second stage of the AFE. The bandpass filter stage consists of an active high-pass filter utilizing the internal op amp (OPA1) in the M0L1306 with 6-MHz gain-bandwidth and an R-C low-pass filter. The high-pass stage makes sure any DC (low frequency) interference is removed (attenuated) without disturbing the modulated signal. The low-pass stage provides filtering to any high-frequency noise presented in the previous signal chain before demodulation. The high-pass filter gain and 3-dB high-pass pole frequency are given as:

$$G_{\text{HPF}} = \frac{C_{0\text{HPF}}}{C_{1\text{HPF}}} = 4.5, \quad f_{3\text{dB,HPF}} = \frac{1}{2\pi C_{1\text{HPF}} R_{\text{HPF}}} = 70.7 \text{ kHz} \quad (5)$$

The 3-dB low-pass frequency is given as:

$$f_{3\text{dB,LPF}} = \frac{1}{2\pi C_{\text{LPF}} R_{\text{LPF}}} = 318.9 \text{ kHz} \quad (6)$$

The bias voltage of the BPF is selected as 1.65 V ($V_{\text{DD}}/2$) generated by two 10-M Ω series resistors as shown in Figure 2-1 and also Figure 2-7.

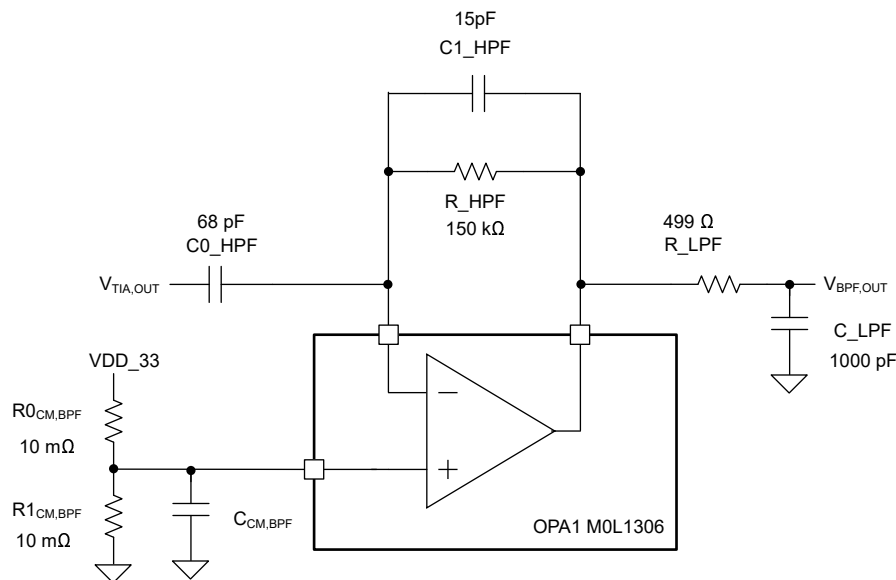


Figure 2-7. BPF Schematic

Figure 2-8 shows the simulated frequency response from input current to BPF output voltage of the combined TIA and BPF stages with the aforementioned design parameters. The peak gain is 118.3 dB (0.82 M Ω) at 144.5 kHz which is lower than the calculated gain of $4.5 \times 249 \text{ k}\Omega = 1.12 \text{ M}\Omega$ due to the low damping factor of the simple poles and the spacing of the cutoff frequencies being less than one decade or more apart. The 3-dB bandpass cutoff frequency is at 56 kHz at the low side and 332 kHz at the high side. The frequency response shape can be simply modified by adjusting corresponding R, C values to satisfy specific design requirements on different modulation frequency selections.

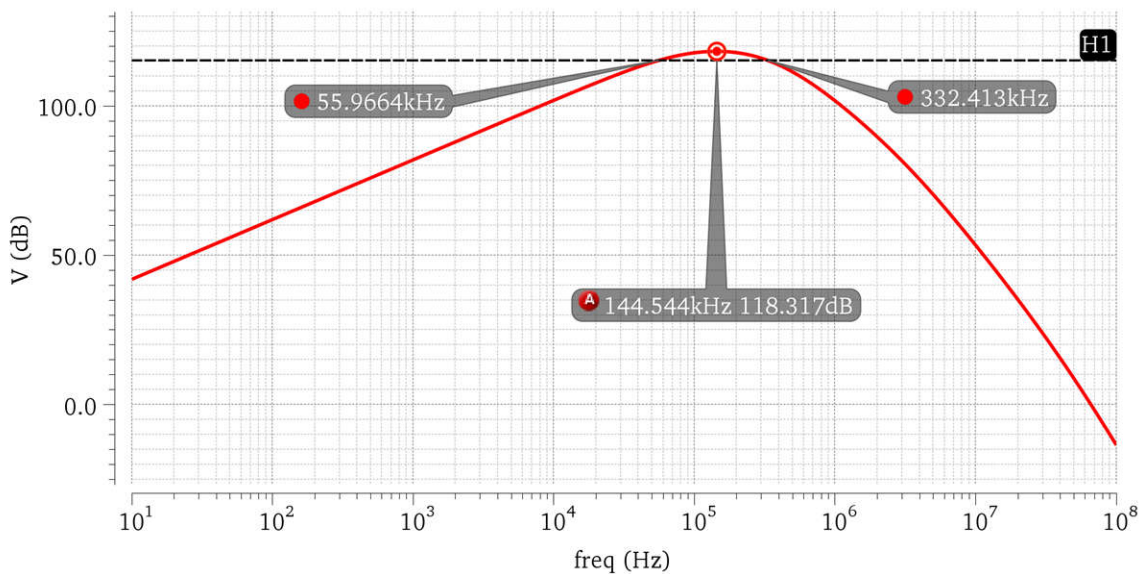


Figure 2-8. Frequency Magnitude Response of Combined TIA and BPF

2.2.3.3 Demodulator and Integrator

Figure 2-9 shows the schematic of the demodulator and integrator stages. The demodulator (multiplier) topology is selected as a chopping switch using two pairs of SPDT analog switches (TS5A623157). The input of the switches are the BPF output and a buffered common mode voltage (1.65 V), respectively. By alternating switches with the LED_DEMOD and LED_DEMODB signals at frequency f_{mod} , the output polarity of the chopping switch relative to the input can be the same or opposite, essentially multiplying the input by +1 and -1, respectively.

The output of the demodulator is fed into an RC integrator. When the reset switch (SN74LVC1G66) is on, the integrator output is reset to $V_{CM,BPF}$. When the reset switch is turned off (integrator is active), the input voltage of the integrator is converted to current I_{INT} by R_{INT} and charges or discharges the capacitor C_{INT} based on the current polarity. The integrator output is sampled by the ADC before the reset *on* signal pulse by pulse.

The integrator R and C is designed as 28 k Ω and 12 pF, respectively, to have a target gain value calculated as:

$$G_{INT} = \frac{2T_{p,mod}}{R_{INT}C_{INT}} \tag{7}$$

$T_{p,mod}$ is the pulse high duration of the demodulation pulses. The integrator gain is designed to be 16 in this design.

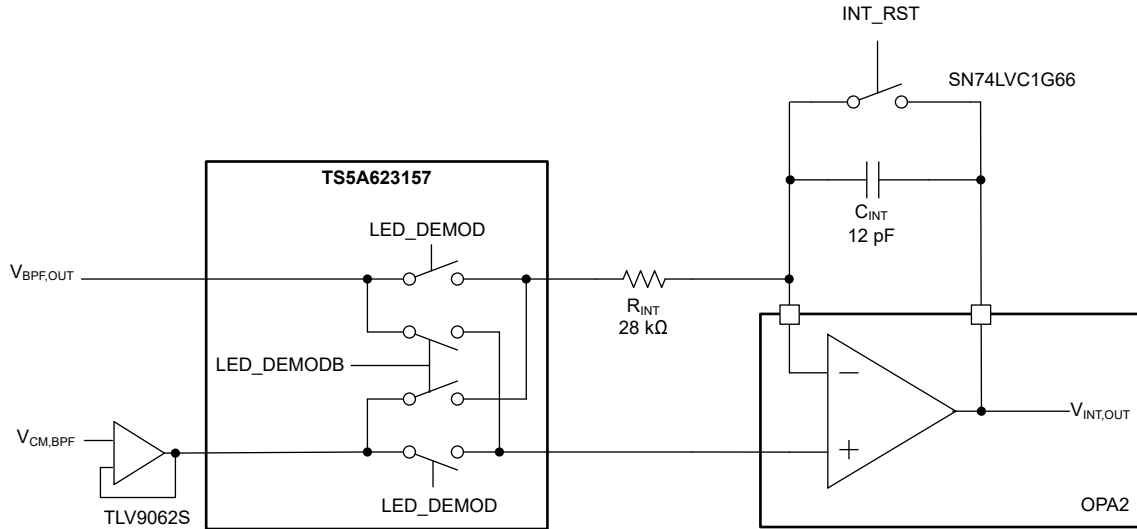


Figure 2-9. Demodulator and Integrator Schematic

Figure 2-10 shows the overall transient waveform of the signal chain when smoke sensing is operated. The digital sample $D_{n,k}$ denotes the sensing signal of the k -th pulse in n -th sensing phase. The final output signal for the single sensing phase can be obtained by passing all the pulses into a digital filter or simply averaging the results. For example, if M is the total number of pulses sent in the given sample phase, the final output is given as:

$$D_n = \frac{\sum_{k=1}^M D_{n,k}}{M} \tag{8}$$

Equation 8 indicates that low noise (better performance) can be achieved by sending a higher number of pulses at the cost of power consumption.

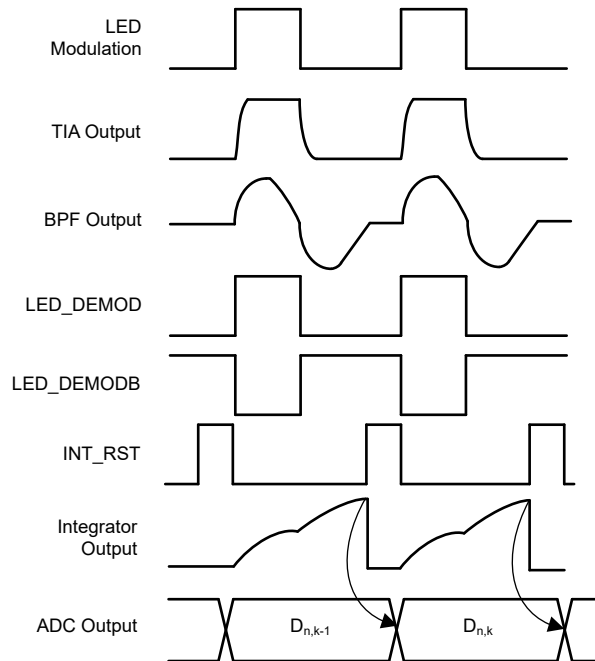


Figure 2-10. Transient Waveform of Intermediate Signal and Control of the Signal Chain

2.2.3.4 LED Driver

Figure 2-11 shows the schematic of the LED drive. The transistors are controlled by the modulation signals LED_BL_MOD and LED_IR_MOD to turn the LEDs on and off. The limiting resistors R_BL and R_IR are designed to have nominal LED current as:

$$I_{LED,IR} = \frac{V_{DD,LED} - V_{F,IR}}{R_{IR}} = \frac{5 - 1.35}{38.3} = 95.3 \text{ mA}, \quad I_{LED,BL} = \frac{V_{DD,LED} - V_{F,BL}}{R_{BL}} = \frac{5 - 3}{100} = 20 \text{ mA} \quad (9)$$

The IR and BLUE LEDs are selected as TSAL6100 and C503B-BAN, respectively. The typical forward voltage, V_F , in the respective data sheets is used in Equation 9 to calculate nominal LED current. The supply voltage, $V_{DD,LED}$ is a regulated output of 5 V, derived from the battery by TPS7A2405, which helps maintain a consistent LED current and smoke sensitivity consequently. If a different LED current is desired, the current-limiting resistors can be replaced accordingly.

As the LED current is not regulated from a constant current source, the output power from the blue and IR LEDs varies across temperature. This results in a signal chain gain variation across temperature. This variation can be addressed by temperature compensation in digital post-processing of the signal chain output by monitoring the ambient temperature using either or both of the onboard temperature sensors of the MOL MCU and the HDC2010.

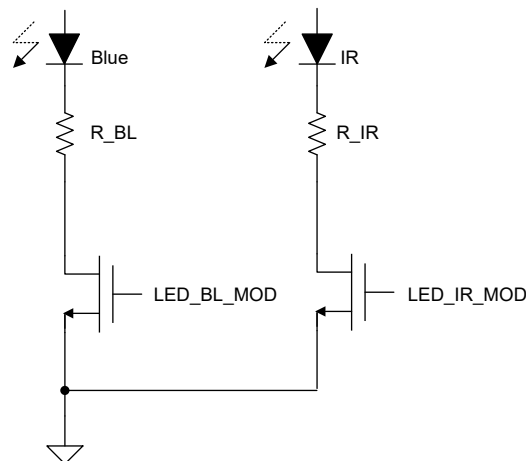


Figure 2-11. LED Driver Schematic

2.2.4 Optical and Mechanical Design

This section covers the customized optical front end and mechanical design. A 2-LED (1 BLUE + 1 IR) and 1-PD design is adopted to enable the smoke type analysis and reduce the false alarm of the smoke detection due to nuisance sources. Figure 2-12 shows a top-down view of the module board to illustrate the arrangement of the optical elements. The angle between the IR LED (TSAL6100) and the PD (SFH213) is forward 125 degrees. The angle between the BLUE LED (C503B-BAN) and the PD is backward 30 degrees, which is specifically designed to leverage both BLUE and IR sensing data to perform analysis of the smoke type. The through-hole optical parts are first inserted into a customized 3D-printed container and soldered onto the top side of the sensing board. The bottom side of the sensing board contains a 9-V battery socket, sensing electronics, LED indicator for smoke alarm, and connectors for communication. Figure 2-13 shows the picture of the top-down view of the bottom side of the board.

A 3D-printed top cover is attached to the top-side of the board (the same side of the optical front end) to block environmental interference such as insects and ambient light, providing a tractable smoke sensing environment. To obtain the best optical performance, the printed cover is spray-painted with matte black paint to reduce the stray-light reflection from the cover. Figure 2-14 shows the complete view of the smoke detector module with cover. Download the 3D step files of these mechanical designs from the TIDA-010941 tool folder.

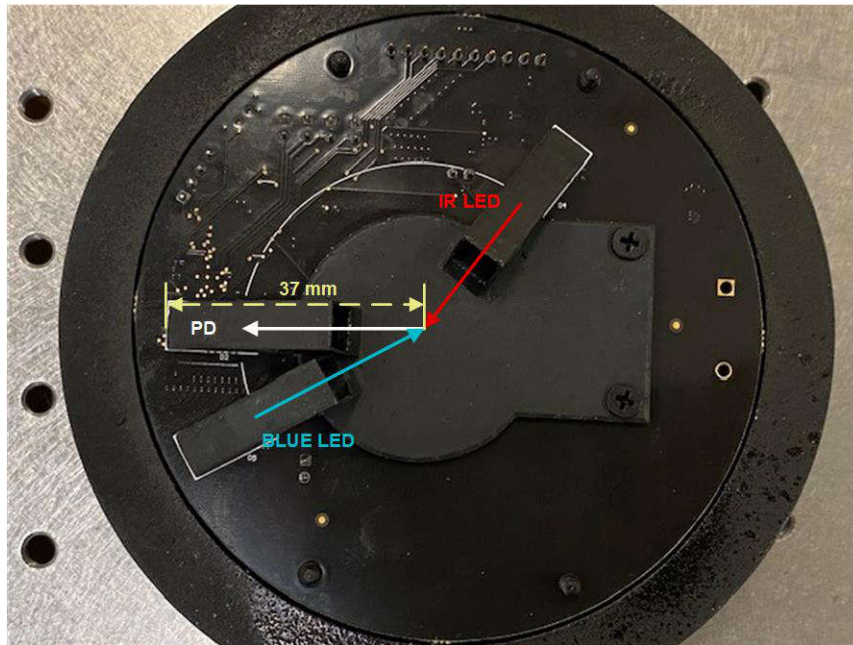


Figure 2-12. Top-Down View of the Optical Front End With Sensing Board

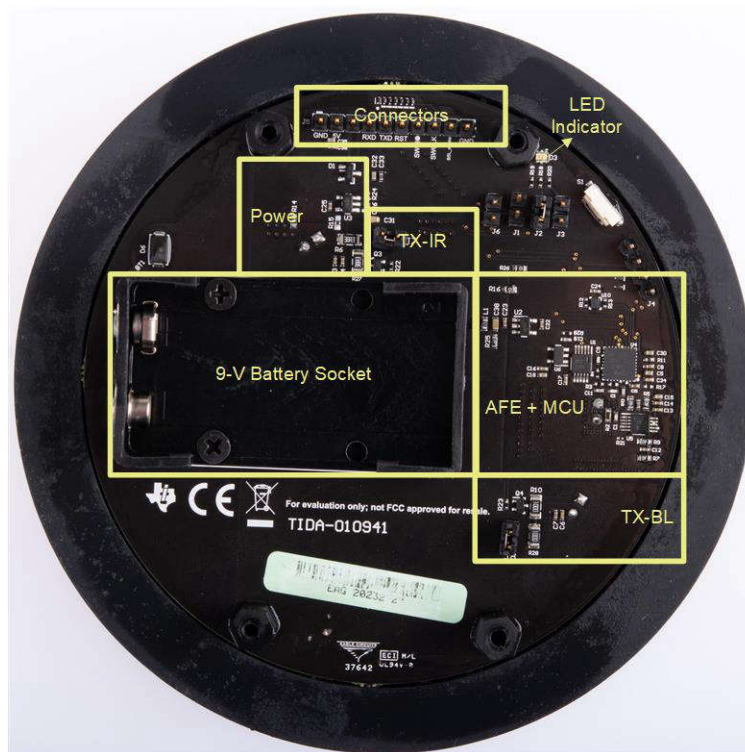


Figure 2-13. Top-Down View of the Bottom-Side Sensing Board



Figure 2-14. Complete View of Smoke Detector Module

2.3 Highlighted Products

2.3.1 MSPM0L1306

MSPM0L134x and MSPM0L130x microcontrollers (MCUs) are part of the highly-integrated, ultra-low-power [32-bit MSPM0 MCU family](#) based on the enhanced Arm® Cortex®-M0+ core platform operating at up to 32-MHz frequency. These cost-optimized MCUs offer high-performance analog peripheral integration, support extended temperature ranges from -40°C to 125°C , and operate with supply voltages ranging from 1.62 V to 3.6 V.

The MSPM0L134x and MSPM0L130x devices provide up to 64KB embedded flash program memory with up to 4KB SRAM. These MCUs incorporate a high-speed on-chip oscillator with an accuracy up to $\pm 1.2\%$, eliminating the need for an external crystal. Additional features include a 3-channel DMA, 16- and 32-bit CRC accelerator, and a variety of high-performance analog peripherals such as one 12-bit 1.68-MSPS ADC with configurable internal voltage reference, one high-speed comparator with built-in reference DAC, two zero-drift zero-crossover operational amplifiers with programmable gain, one general-purpose amplifier, and an on-chip temperature sensor. These devices also offer intelligent digital peripherals such as four 16-bit general purpose timers, one windowed watchdog timer, and a variety of communication peripherals including two universal asynchronous receivers, transmitters (UART), one SPI, and two I²Cs. These communication peripherals offer protocol support for LIN, IrDA, DALI, Manchester, Smart Card, SMBus, and PMBus.

The TI MSPM0 family of low-power MCUs consists of devices with varying degrees of analog and digital integration allowing customers to find the MCU that meets the needs of the project. The architecture combined with extensive low-power modes are optimized to achieve extended battery life in portable measurement applications.

MSPM0L134x and MSPM0L130x MCUs are supported by an extensive hardware and software ecosystem with reference designs and code examples to get the design started quickly. Development kits include a LaunchPad™ Development Kit available for purchase and design files for a Target-Socket Board. TI also provides a free MSP Software Development Kit (SDK), which is available as a component of Code Composer Studio™ IDE desktop and cloud version within the [TI Resource Explorer](#). MSPM0 MCUs are also supported by extensive online collateral, training with [MSP Academy](#), and online support through the [TI E2E™ support forums](#).

For complete module descriptions, see the [MSPM0 L-Series 32-MHz Microcontrollers](#) Technical Reference Manual.

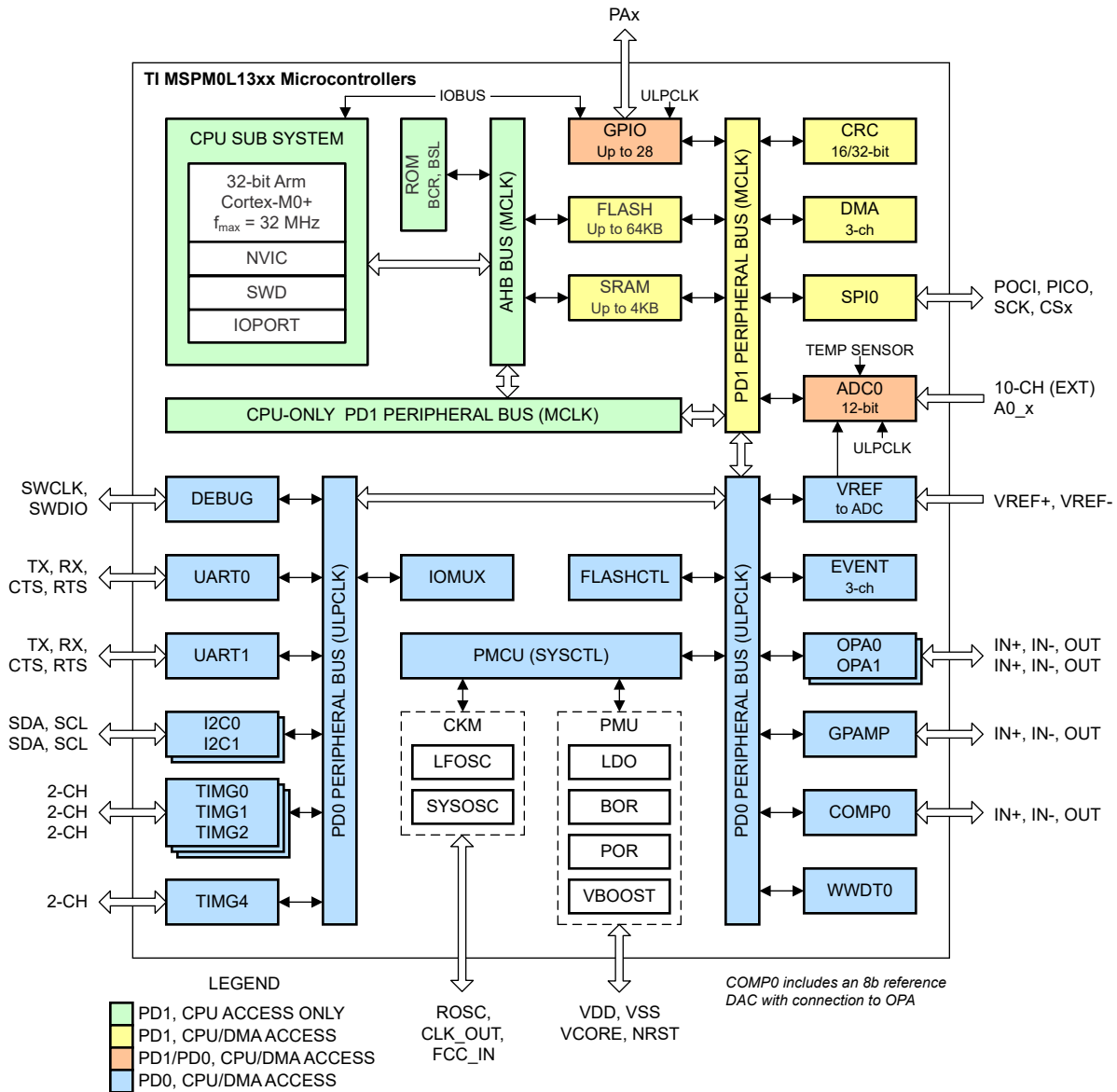


Figure 2-15. MSPM0L130x Functional Block Diagram

2.3.2 TLV9062S

The TLV906x devices are a family of low-power, rail-to-rail input and output op amps. These devices operate from 1.8 V to 5.5 V, are unity-gain stable, and are designed for a wide range of general-purpose applications. The input common-mode voltage range includes both rails and allows the TLV906x series to be used in virtually any single-supply application. Rail-to-rail input and output swing significantly increases dynamic range, especially in low-supply applications. The high bandwidth enables this family to drive the sample-and-hold circuitry of analog-to-digital converters (ADCs).

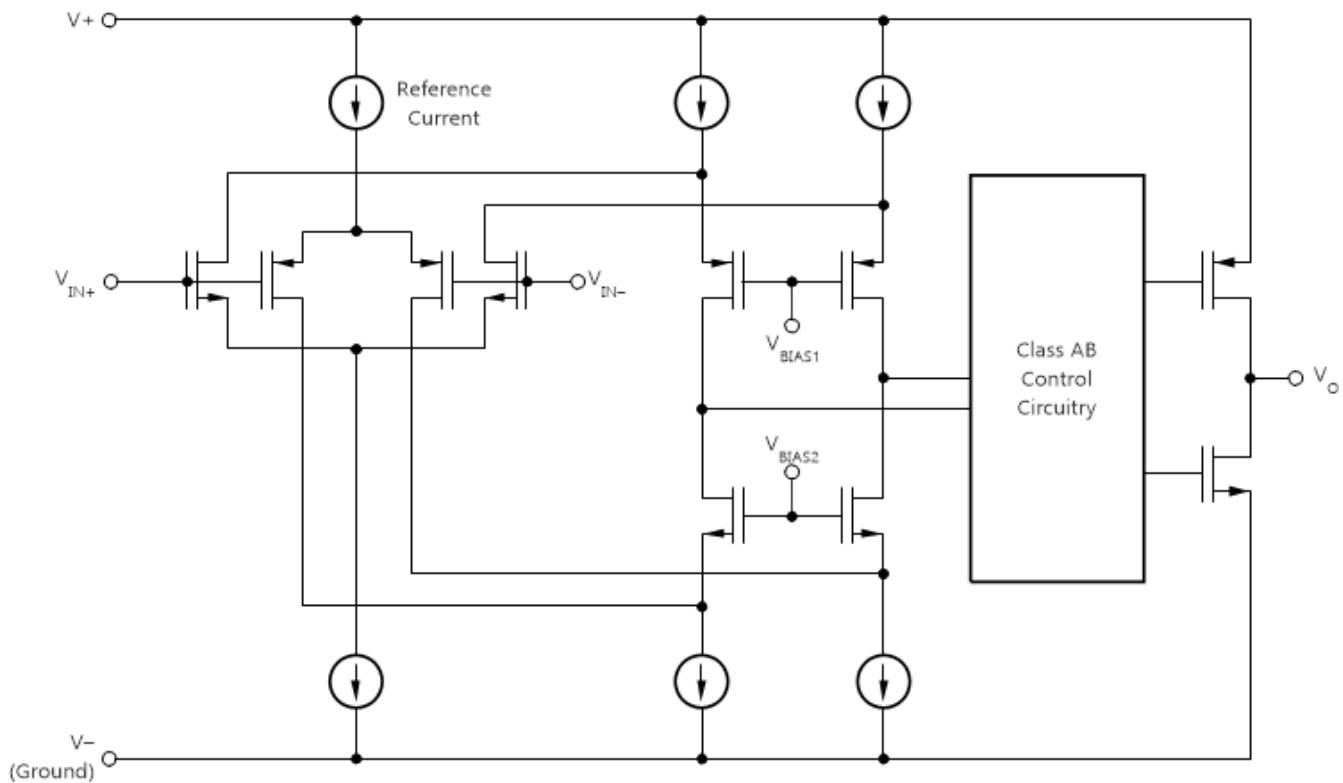


Figure 2-16. TLV9062 Functional Block Diagram

2.3.3 TPS7A24

The TPS7A24 is an 18-V, low quiescent current, low-dropout (LDO) linear regulator. The low I_Q performance makes the TPS7A24 an excellent choice for battery-powered or line-power applications that are expected to meet increasingly stringent standby-power standards. The fixed-output versions have the advantage of providing better accuracy with fewer external components, whereas the adjustable version has the flexibility for a far wider output voltage range.

The 1.25% accuracy over temperature makes this device an excellent choice for meeting a wide range of microcontroller power requirements.

For increased reliability, the TPS7A24 also incorporates overcurrent, overshoot pulldown, and thermal shutdown protection. The operating junction temperature is -40°C to $+125^{\circ}\text{C}$, and adds margin for applications concerned with higher working ambient temperatures.

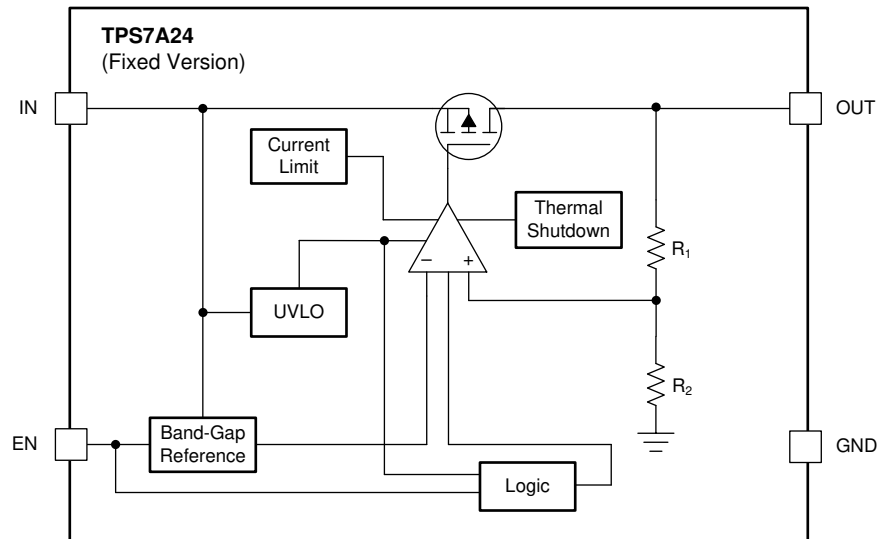
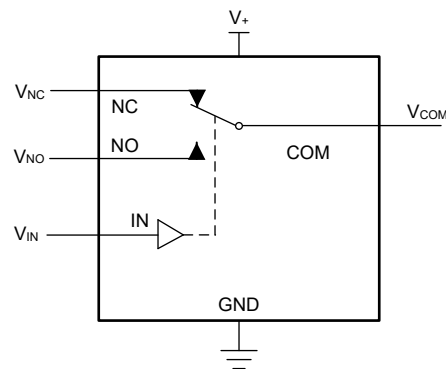


Figure 2-17. TPS7A24 Fixed Version Block Diagram

2.3.4 TS5A623157

The TS5A623157 is a dual single-pole, double-throw (SPDT) analog switch designed to operate from 1.65 V to 5.5 V. This device can handle both digital and analog signals. Signals up to V_+ (peak) can be transmitted in either direction.

The TS5A623157 senses overshoot and undershoot events at the I/Os and responds by preventing voltage differentials from developing and turning the switch on.



FUNCTION TABLE

IN	NC TO COM, COM TO NC	NO TO COM, COM TO NO
L	ON	OFF
H	OFF	ON

Figure 2-18. TS5A623157 Block Diagram

2.3.5 SN74LVC1G66

This single analog switch is designed for 1.65-V to 5.5-V VCC operation.

The SN74LVC1G66 device can handle analog and digital signals. The device permits bidirectional transmission of signals with amplitudes of up to 5.5 V (peak). Like all analog switches, the SN74LVC1G66 is bidirectional.

NanoFree package technology is a major breakthrough in IC packaging concepts, using the die as the package.

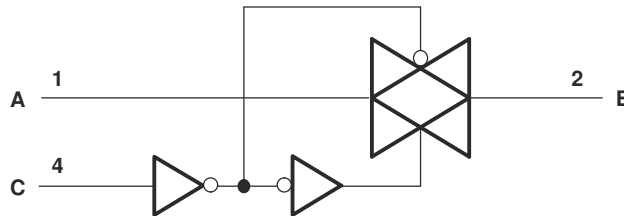


Figure 2-19. SN74LVC1G66 Functional Block Diagram

2.3.6 HDC2010

The HDC2010 is a highly-integrated digital humidity and temperature sensor that incorporates both humidity sensing and temperature-sensing elements, an analog-to-digital converter, calibration memory, and an I2C interface that are all contained in a 1.5-mm × 1.5-mm DSBGA package. The HDC2010 provides excellent measurement accuracy with very low power consumption and features programmable resolution for both humidity and temperature:

- Temperature resolution [9, 11, 14]
- Humidity resolution [9, 11, 14]

The conversion time during measurements is dependent upon the configured resolution for humidity and temperature, which can be configured for the best available power consumption.

The HDC2010 device incorporates a state-of-the-art polymer dielectric to provide capacitive-sensing measurements. As with most relative humidity sensors that include this type of technology, the user must meet certain application requirements to make sure of the best device performance for the sensing element. The user must:

- Follow the correct storage and handling procedures during board assembly. See the [Humidity Sensor: Storage and Handling Guidelines](#) application report for these guidelines.
- Protect the sensor from contaminants during board assembly and operation.
- Reduce prolonged exposure to both high temperature and humidity extremes that can impact sensor accuracy.
- Follow the correct layout guidelines for best performance. See the [Optimizing Placement and Routing for Humidity Sensors](#) application report for these guidelines.

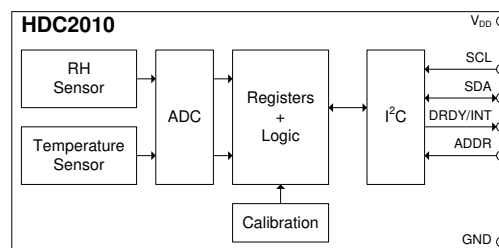


Figure 2-20. HDC2010 Functional Block Diagram

3 Hardware, Software, Testing Requirements, and Test Results

3.1 Hardware Requirements

3.1.1 Power

The default option of the smoke detection module board is to install a 9-V battery in the battery socket. Once the power is on, the module starts operation automatically.

The user can also use an external 5-V supply to power the board. To achieve this complete the following:

- Remove the 0- Ω resistor at R15 location and install a 0- Ω resistor at R14 location
- Connect GND and 5-V connector to the external ground and external supply, respectively

3.1.2 Communication Interface

The module also provides the interface for data communication and re-programming. To do this, connect the connector J5 (GND, RXD, TXD, NRST, SWDIO, SWCLK, and BSL) to the J101 (XDS110-ET Debug Probe domain) connector on the [LP-MSPM0L1306](#) LaunchPad Development Kit as [Figure 3-1](#) shows.

The XDS110-ET provides a *back-channel* UART-over-USB connection with the host, which can be very useful during debugging and for easy communication with a PC. This interface is used by the GUI described in [Section 3.2.4](#) as well for receiving signal chain output data for post-processing on a PC. Connect RXD and TXD for application UART communication.

Connect NRST (Reset signal), SWDIO (serial wire debug data signal), SWCLK (serial wire debug clock signal) and BSL (bootstrap loader signal) for programming and debugging. More details related to those jumpers are found in the [MSPM0L1306 LaunchPad Development Kit \(LP-MSPM0L1306\)](#) user's guide.

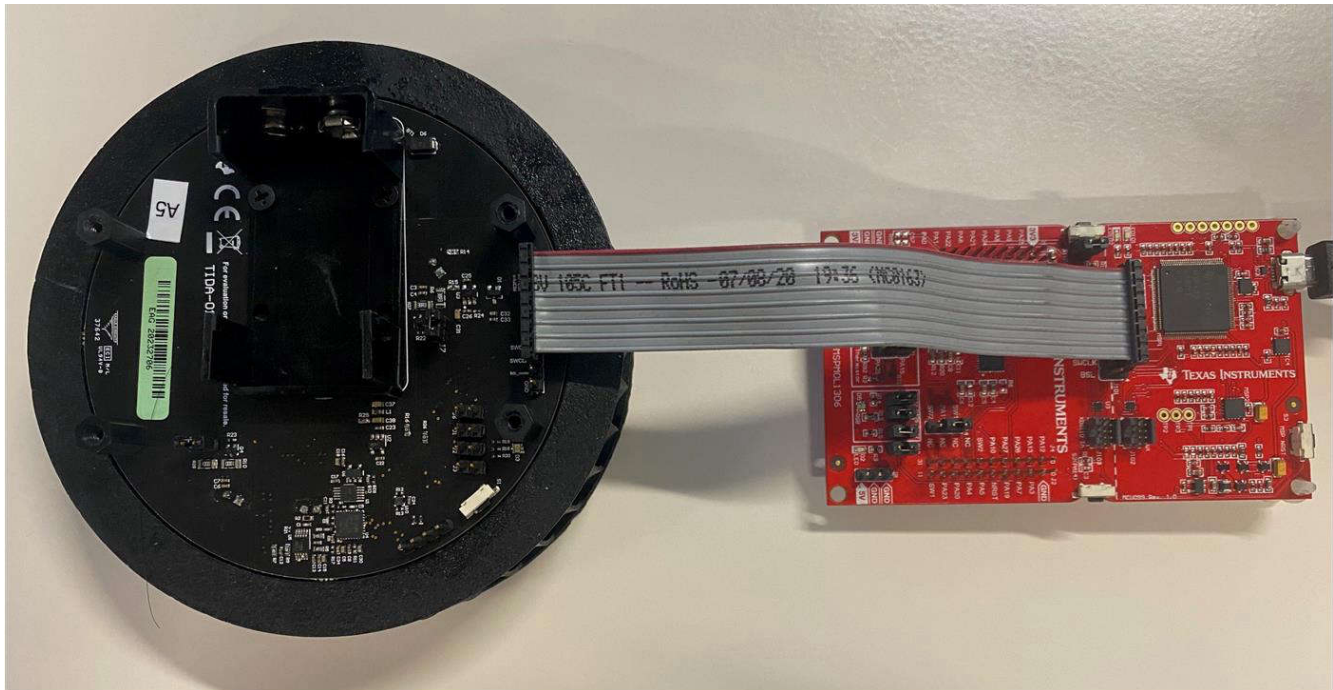


Figure 3-1. Connection Between SASI Smoke Detection Module and LP-MSPM0L1306

3.1.3 Headers

The J1, J2, and J3 connectors are provided to enable the RGB LED indication on the board. J2 (red LED) is enabled (connected) by default for smoke detection indication. The Blue and Green LEDs enabled by connectors J2 and J3 are currently not being used in firmware.

The J4 connector is for extra general-purpose input/output (GPIO) or a GND probe.

Pin PA18 of the MCU is shared for both the Bootstrap Loader (BSL) function and the analog input OPA1_IN0+. When BSL is not in use, J6 connector is disconnected by default. Likewise, when the BSL signal is being used, connect J6.

The J7 and J8 connectors (connected by default) are provided to reduce the Blue and IR LED current by disconnecting them as shown in Figure 3-2.

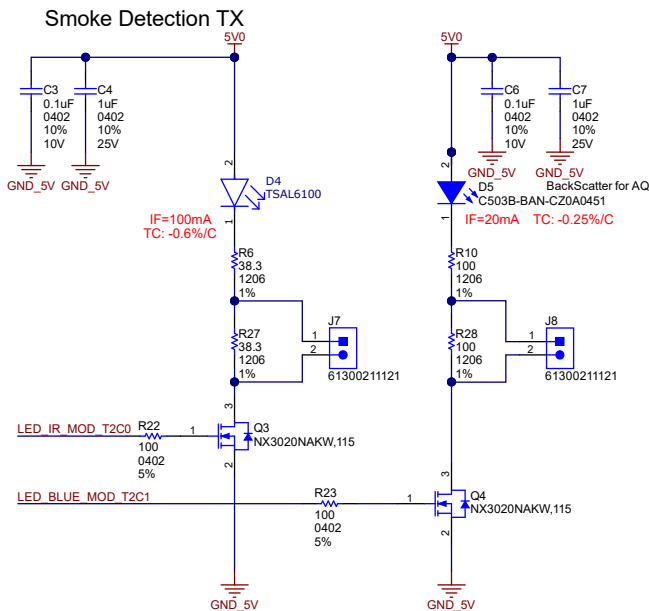


Figure 3-2. LED Schematic With Current Reduction Function Using J7 and J8

3.2 Software Requirements

3.2.1 Getting Started Firmware

The firmware for this reference design is released as [Demonstration application examples](#) and are available in the latest [MSPM0 SDK](#). An optional Python® graphical user interface (GUI) allows developers to adjust the Blue and IR LED threshold values and observe the system response. The GUI is available at [TIDA-010941](#).

The demonstration application examples can be evaluated online using the cloud version of CCS Theia, known as [CCS Cloud IDE](#), or offline using the desktop versions of [CCS Theia](#) or [CCS Eclipse](#), a legacy IDE.

The cloud version of CCS Theia is referred to as CCS Cloud IDE or CCS Cloud throughout the document.

To evaluate the demonstration application examples online using CCS Cloud, follow the steps below:

1. Open the MSPM0 SDK in [TI Developer Zone](#).
2. Navigate to the *SASI Smoke Detector* examples directory by clicking Examples->Development Tools->LP-MSPM0L1306->SASI Smoke Detector. Click the 3 dots at the right side of the example, and click *Import to CCS Cloud IDE*.

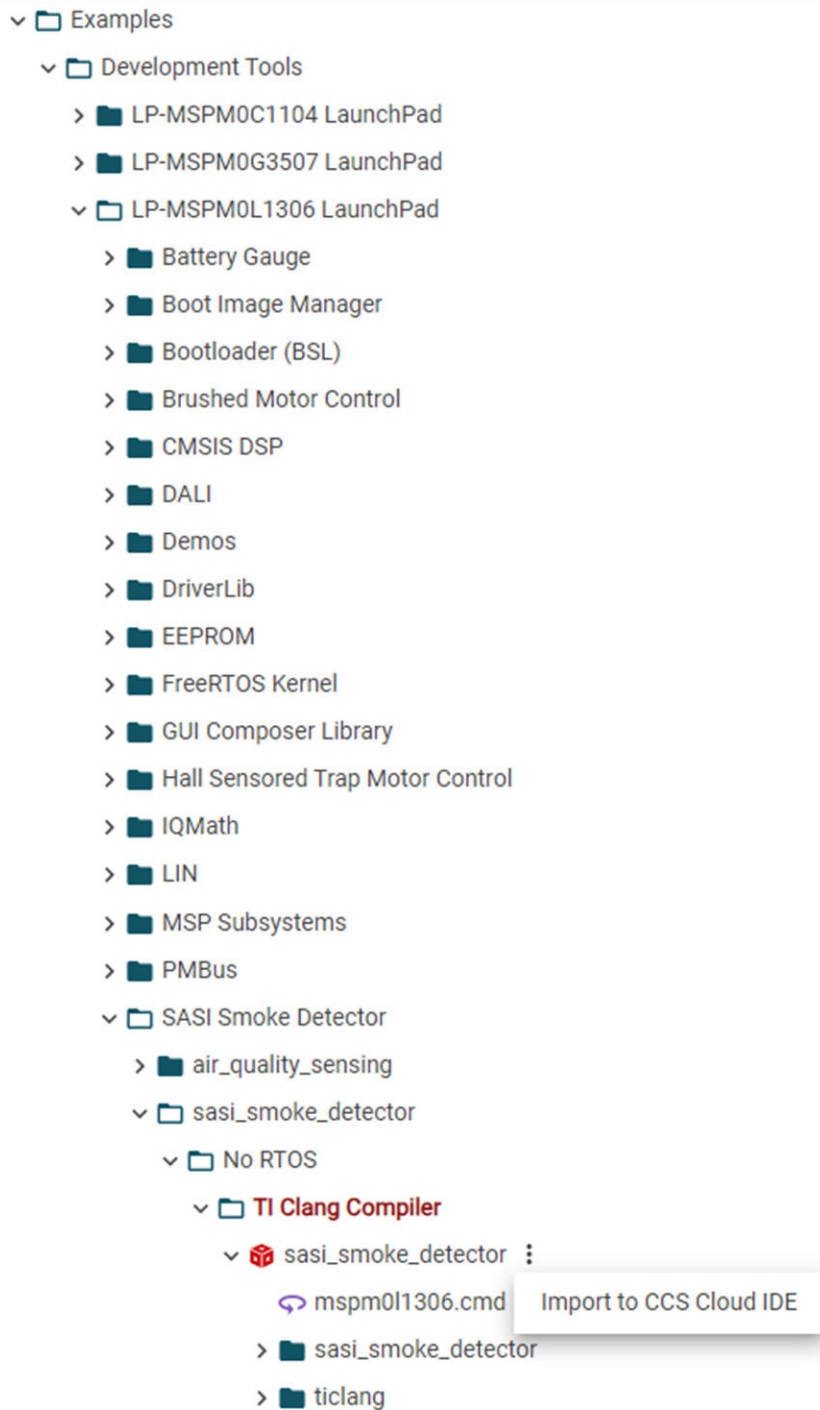


Figure 3-3. Firmware Demonstration Example SDK Directory Path

3. After importing the examples to the CCS Cloud IDE, the project explorer window appears as follows:

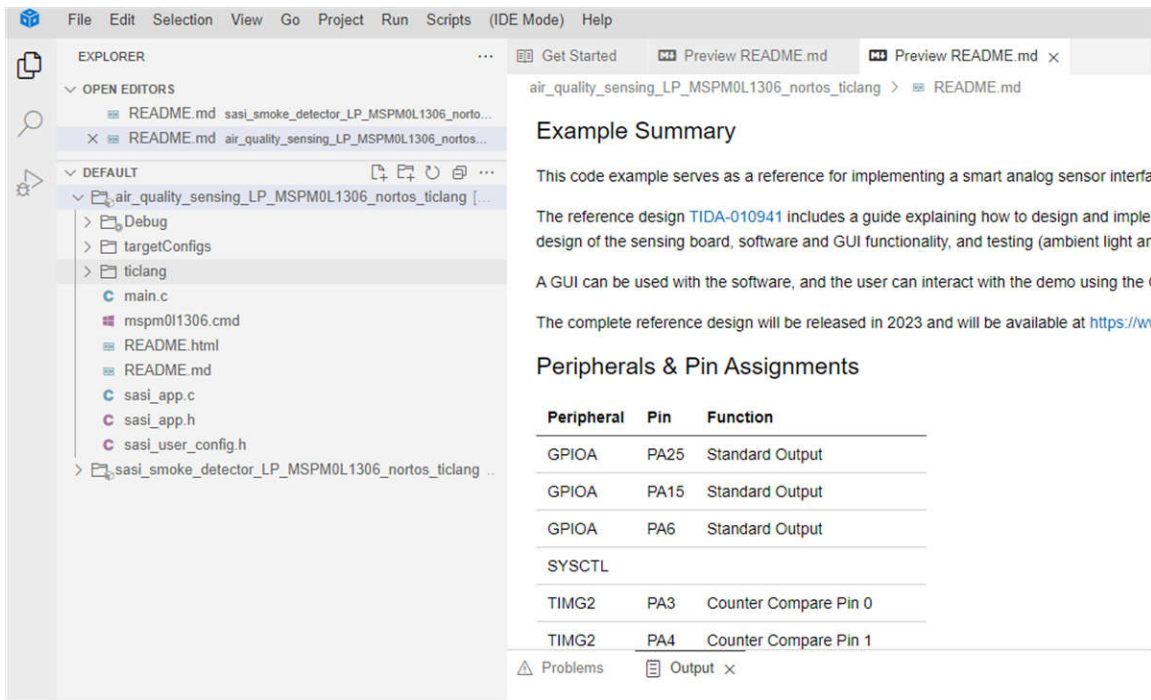


Figure 3-4. CCS Cloud IDE After Firmware Demonstration Example Import

- The imported examples can be built and loaded onto the device as normal. See the [Code Composer Studio Theia User's Guide](#) for more details and instructions on using the cloud and desktop versions of CCS Theia.

To evaluate the demonstration application examples offline using the desktop versions of CCS Theia or CCS Eclipse, see the [MSPM0 SDK QuickStart Guide for CCS](#) and the [MSPM0 SDK QuickStart Guide for CCS Theia](#) for import instructions into those tools.

Developers can use these code examples as references for implementing a smoke detector or air-quality sensing system using the Smart Analog Sensor Interface (SASI) sensing board.

3.2.2 Measurements and Smoke Detection

This section introduces the reference software design of the smoke detector module. [Figure 3-5](#) shows the power-on sensing sequence.

Once power is on, the smoke detector enters an 8-second calibration state to obtain a baseline signal for sensing. During the calibration state, the smoke detector must be placed in a clean-air environment to make sure the calibration is properly performed. Recalibration can always be accomplished by power-cycling or using either the software reset function or hardware reset button provided. The calibration is only required for correct smoke detection using the predefined detection algorithm and threshold. If only raw signals are of interest, the calibration is not required.

After calibration, the smoke sensing is performed in a duty-cycled fashion. During sleep phase, all sensing circuitry as well as peripherals of the M01306L are disabled and the M01306L is in standby mode to conserve energy. [Figure 3-6](#) illustrates this duty-cycled sensing scheme. The sensing period can be updated on-the-fly as necessary for either energy saving or sensing rate performance.

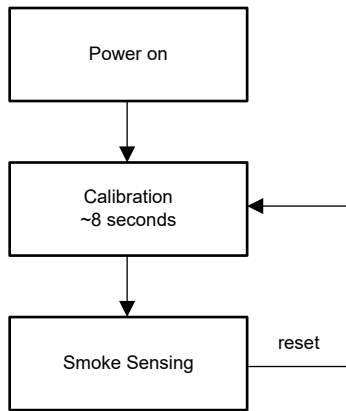


Figure 3-5. Power-on Sensing Sequence With Calibration

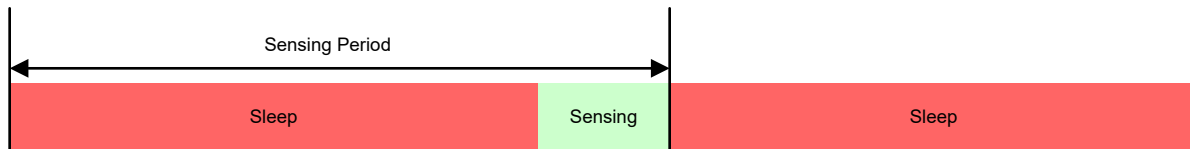


Figure 3-6. Simplified View of Smoke Sensing Timing Diagram

Figure 3-7 shows the simplified smoke detection algorithm that is programmed in M0L1306. There are two power modes defined in the software: low-power and high-power mode. The smoke detector starts with low-power mode after power on and calibration state. The low-power mode has a low number of pulses and low sensing rate. An early-warning threshold TH_0 is set to determine whether high-power mode and actual smoke detection is operated. In high-power mode, a higher number of pulses and high sensing rate is adopted. Table 3-1 shows the default configuration of low and high-power modes. Once the IR signal surpasses the TH_0 threshold, an adaptive threshold TH_{adp} is calculated based on both the IR and BLUE signals. If the IR signal surpasses the TH_{adp} threshold, the alarm count increments. A smoke detected alarm is triggered after $NALARM$ times of consecutive alarm count increment.

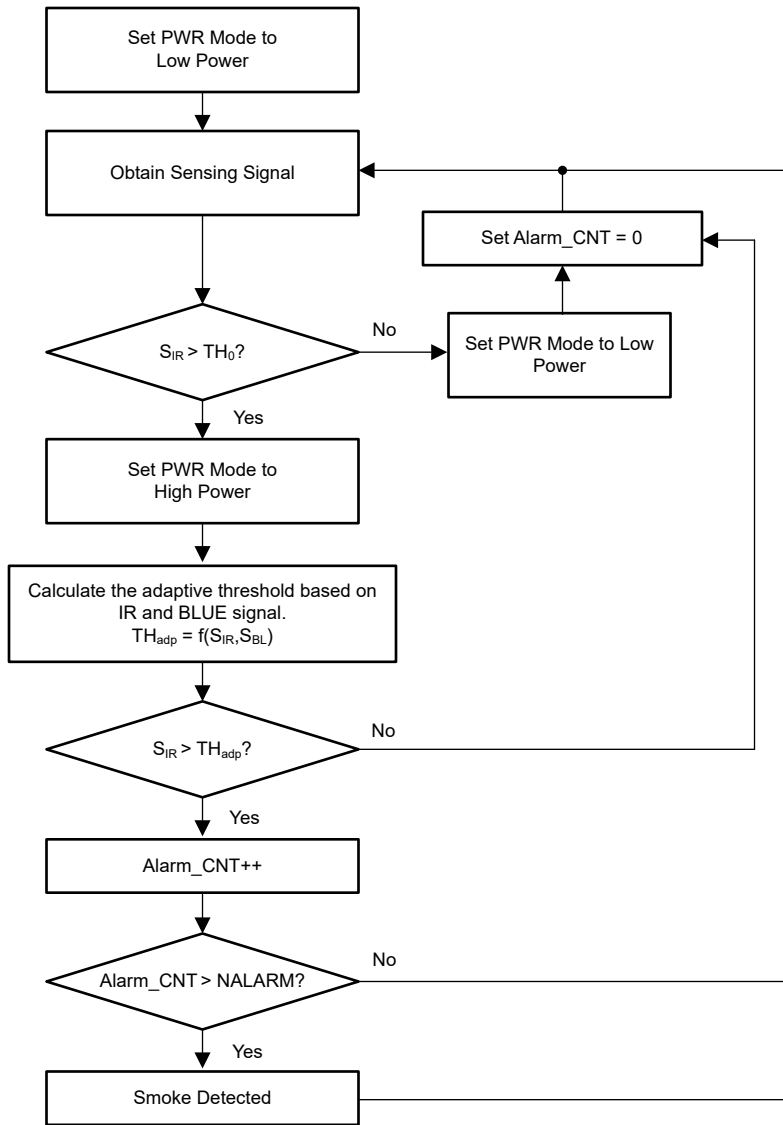


Figure 3-7. Flow Chart of Built-in Smoke Detection Algorithm

Table 3-1. Configuration of Different Power Modes

PARAMETER	LOW-POWER MODE	HIGH-POWER MODE
Sensing Period (s)	10	1
# of Pulses	16	300

The reference design software also provides user-configuration parameters located in the `sasi_user_config.h` file. The details of configurable parameters are provided in [Table 3-2](#).

Set the measurement period parameters `SASI_RTC_PRD_MS` no less than $0.173 \times \text{SASI_N_VSIG_PULSES} + 5$ if UART data transmission is disabled. If UART data transmission is enabled, have `SASI_RTC_PRD_MS` no less than 400 to secure the data transmission.

`SASI_N_VSIG_PULSES` selection can be determined based on the power and noise requirements in each mode. Increasing the value of `SASI_N_VSIG_PULSES` results in lower noise and increased power consumption. The minimum and maximum values of `SASI_N_VSIG_PULSES` that is supported is 4 and 300, respectively.

`N_CAL_START` is determined by the settling time of the signal chain after start-up or reset. Make sure `N_CAL_START` is no less than $5000 / \text{SASI_RTC_PRD0_MS}$ for at least 5 seconds of settling time.

It is possible to set both SASI_RTC_PRD0_MS and SASI_N_VSIG_PULSES0 to different values than SASI_RTC_PRD2_MS and SASI_N_VSIG_PULSES2, respectively, for the start-up calibration mode. However, to provide reliable smoke detection, set SASI_RTC_PRD0_MS and SASI_N_VSIG_PULSES0 to be equal to the respective high-power mode sensing parameters, SASI_RTC_PRD2_MS and SASI_N_VSIG_PULSES2.

Table 3-2. User-Configurable Parameters

PARAMETER NAME	DESCRIPTION	DEFAULT VALUE
SASI_RTC_PRD0_MS	Measurement period for start-up calibration in milliseconds	1000
SASI_RTC_PRD1_MS	Measurement period for low-power mode sensing in milliseconds	10000
SASI_RTC_PRD2_MS	Measurement period for high-power mode sensing in milliseconds	1000
SASI_N_VSIG_PULSES0	Number of signal pulses for start-up calibration	300
SASI_N_VSIG_PULSES1	Number of signal pulses for low-power mode sensing	16
SASI_N_VSIG_PULSES2	Number of signal pulses for high-power mode sensing	300
N_CAL_START	Number of measurements to skip after start-up or reset before calibration	6

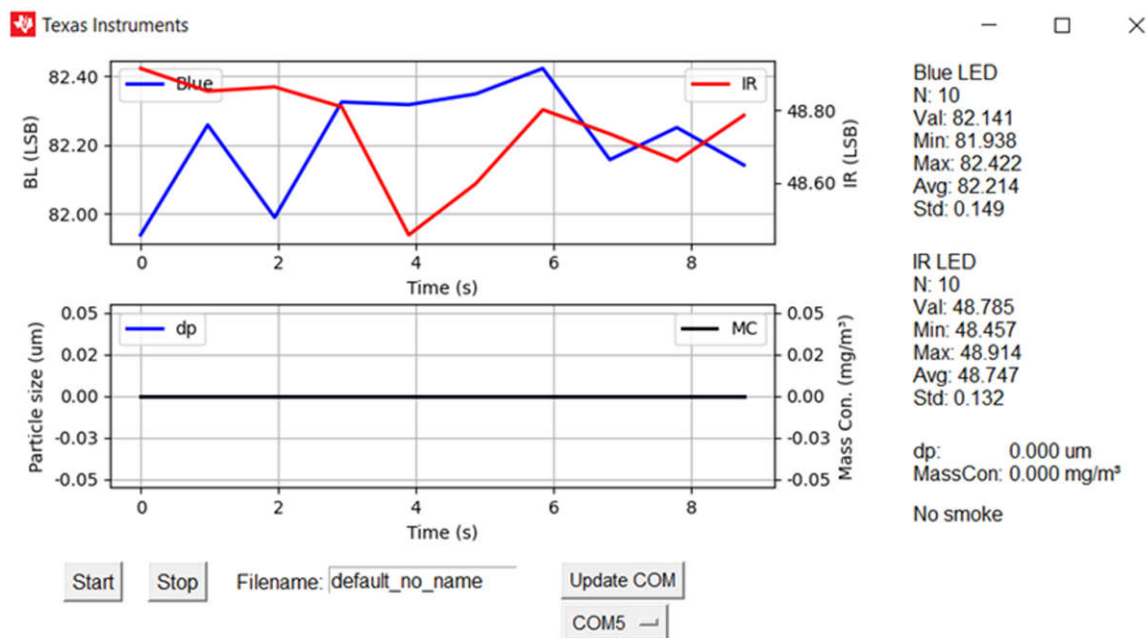
3.2.3 Additional Demonstration Functionality

In addition to implementing a smoke detection algorithm, the software includes the following features:

- Air quality sensing: estimated particle size and mass concentration is also tracked to enable air-quality sensing applications. One of the examples included is a basic demonstration application for air-quality sensing.
- GUI: a GUI is provided to show a visual representation of the measurements. Developers can log the data, view the particle information, and see whether smoke was detected. The GUI also streams the measurements to the terminal and prints time and signal response as well.

3.2.4 Smoke Detector GUI

A GUI developed with Python is included with this reference design. Figure 3-8 shows a screen capture of the GUI. In addition to the graphical view, the data that is displayed is also presented live in a terminal window as shown in Figure 3-9.


Figure 3-8. GUI Screen Capture

```

----Start Measurement----
Time          Count   IR_LSB      BL_LSB      SmokeFlag    dp      MassCon
11:01:35.51   1      48.9141     81.9375     0            0.000  0.000
11:01:36.49   2      48.8516     82.2578     0            0.000  0.000
11:01:37.46   3      48.8633     81.9883     0            0.000  0.000
11:01:38.44   4      48.8086     82.3242     0            0.000  0.000
11:01:39.41   5      48.4570     82.3164     0            0.000  0.000
11:01:40.38   6      48.5977     82.3477     0            0.000  0.000
11:01:41.36   7      48.8008     82.4219     0            0.000  0.000
11:01:42.33   8      48.7344     82.1563     0            0.000  0.000
11:01:43.31   9      48.6602     82.2500     0            0.000  0.000
11:01:44.28  10     48.7852     82.1406     0            0.000  0.000
Saving figure --> 20231006_default_no_name_COM5_0
----Stop Measurement----

```

Figure 3-9. GUI Terminal Window Output

To use the smoke detector GUI:

1. The smoke detector GUI is distributed via Python source code, and must be built into an executable before use. Unzip the file containing the Python source code, and refer to the accompanying README for instructions on building the GUI.
2. Connect the SASI sensing board to the LaunchPad Development Kit. Only the integrated XDS110 emulator on the LaunchPad is needed for PC communication. The rest of the LaunchPad is not activated.
3. Connect the LaunchPad to the PC via USB cable.
4. Open the GUI `sasi_smoke_detector_m011306.exe`.
 - a. Make sure to start with clean air.
 - b. Wait for 12 seconds after first time power up or reset for proper calculation of base signal.
5. Click the *Update COM* button for COM port auto-detection.
6. Enter the filename for data logging.
 - a. The log file is stored in the `capture\<date>\fo1` folder along with an image of the GUI plot.
 - b. Multiple logs are appended with “_0”, “_1”, and so forth.
 - c. Each file logs 1000 entries, and a new file is generated every 1000 entries.
7. Set the smoke trigger threshold value in the Least Significant Bit (LSB).
8. Click the *Start* button to start measurement.
 - a. Measurement statistics are displayed on the side in LSB.
 - b. Smoke indication (no smoke or smoke detected) is also displayed based on whether the signal exceeds the threshold.
 - c. Estimated particle size and mass concentration are also displayed.
9. Click the *Stop* button to stop measurement.
 - a. Data is automatically logged. Time and signal response in LSB from the IR and Blue LEDs, particle size estimation, and the smoke detection flag are also streamed to the terminal.

3.3 Test Setup

3.3.1 UL217 Smoke Box and Fire Testing Setup

Figure 3-10 and Figure 3-11 show the test setup of smoke box and fire room per UL217, respectively. Sensitivity and directionality tests are performed via smoke box and the remaining fire and nuisance testing are performed via fire room.

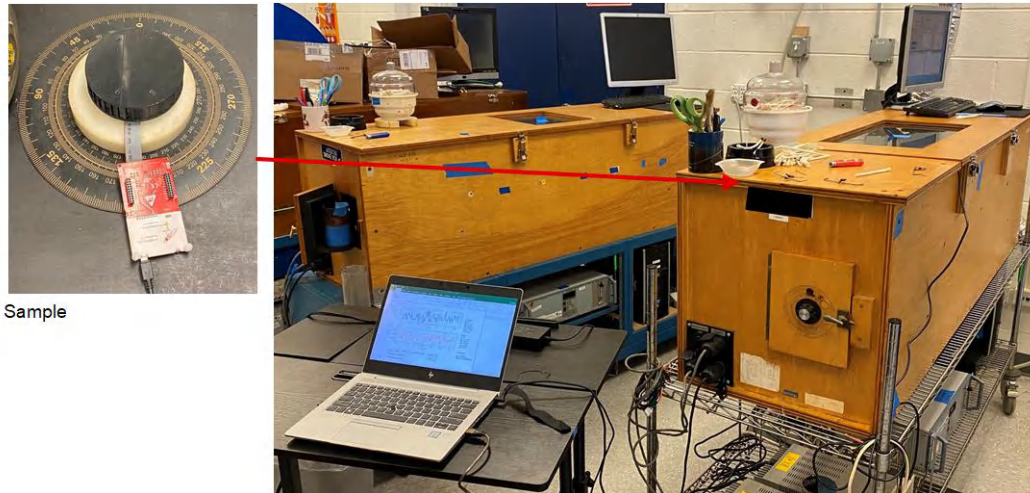


Figure 3-10. Test Setup for Smoke Box Tests per UL217

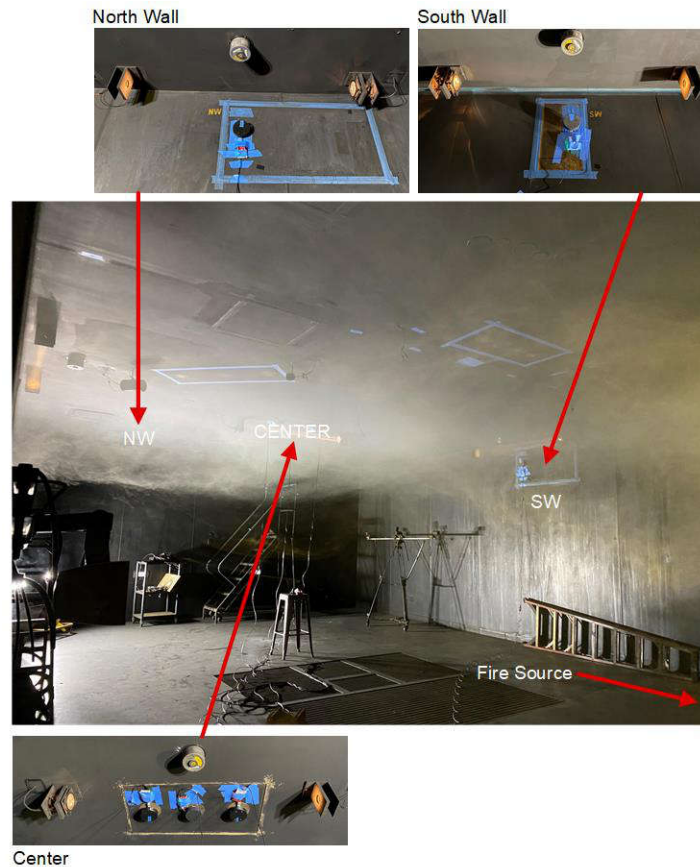


Figure 3-11. Test Setup for Fire Room Tests per UL217

3.3.2 Ambient Light Testing Setup

To evaluate the smoke detection module performance under ambient light, the module samples are tested with testing facility and method subjected to the light stability testing in UL217 (See section 47.1f of the UL217 9th edition). The test setup is shown in [Figure 3-12](#) and results are presented in [Section 3.4.2](#).

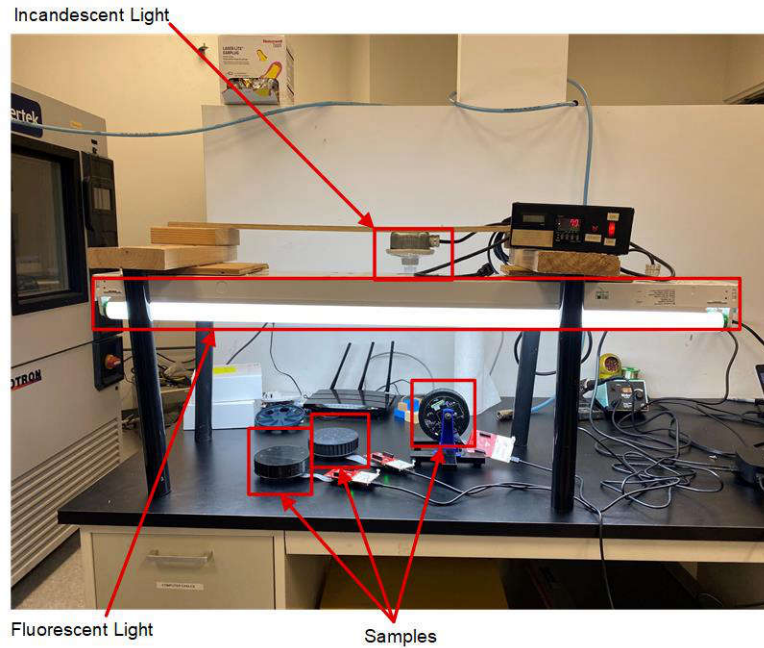


Figure 3-12. Testing Setup of Ambient Light Effects on Smoke Detection Module

3.3.3 Air-Quality Sensing Test Setup

This smoke detection module can also provide the average particle size and mass concentration information based on the dual-beam optical arrangement and algorithms for air-quality sensing applications. To evaluate the accuracy of the size and mass concentration performance, the module output is compared with an off-the-shelf laser-based particulate matter (PM) sensor during real-time particle measurement.

[Figure 3-13](#) shows the testing setup, which includes the aerosol generator and a mixing chamber. The aerosol generator generates atomized aerosol particles with different particle sizes, which is sent to the mixing chamber after a diffusion dryer (not shown in [Figure 3-13](#)). There are two fans running in the mixing chamber to circulate and mix the air. The reference (laser-based PM sensor) and our smoke-detection module are placed at the same level in the chamber to make sure similar air samples are measured.

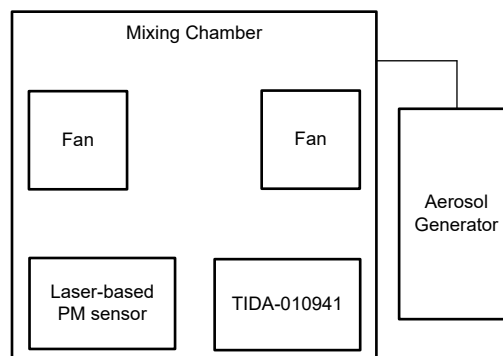


Figure 3-13. Testing Setup of Air-Quality Sensing

3.4 Test Results

3.4.1 UL217 Testing Results

A separate UL217 testing report from third-party testing of the UL217 9th edition Sensitivity and Fire Room tests are included as part of this reference design and can be accessed at [TIDA-010941](#).

3.4.2 Ambient Light Testing Results

Figure 3-14 and Figure 3-15 show the transient response of the smoke detection module for fluorescent and incandescent light conditions with different number of pulses, respectively. For the fluorescent light scenario, the noise performance shows no degradation with 300 pulses. Reducing the number of pulses to 16, larger variations are seen in the panel on the right side of Figure 3-14. This is due to the fact that fluorescent light has interference tones at 44 kHz and the harmonics of the 44 kHz fundamental in the power spectrum, which is close to the modulation frequency. Even though with large variation, the smoke detection module does not trigger a false alarm with a typical threshold of 20 LSB.

Incandescent light interference (main tone at 120 Hz); however, is strongly rejected (> 60 dB) by the bandpass filter in the modulation signal chain. The tests show no significant change of noise performance with the light on and off, even with a 4-pulse scenario.

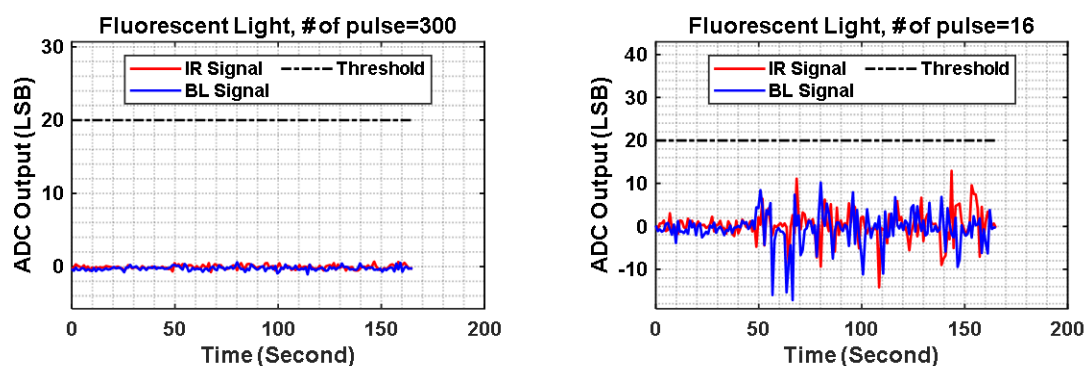


Figure 3-14. Transient Response Output With Fluorescent Light Interference

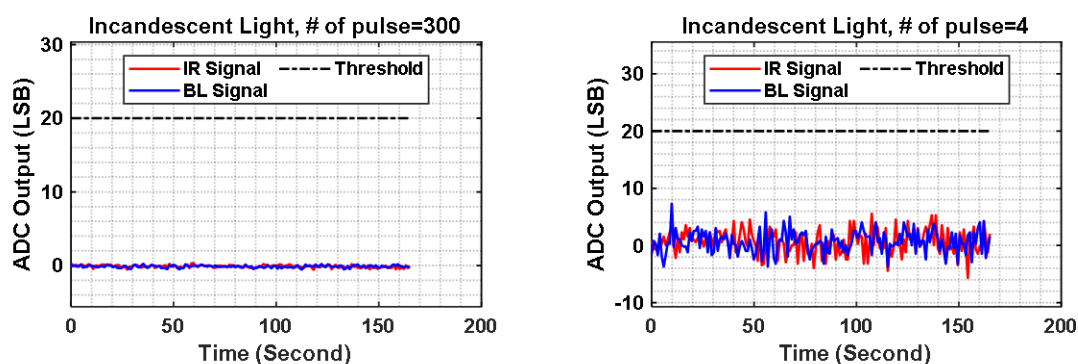


Figure 3-15. Transient Response Output With Incandescent Light Interference

3.4.3 Air-Quality Sensing Test Results

This section shows the air-quality test results of the smoke sensing module with respect to the reference. Figure 3-16 shows the real-time averaged particle size reading of the smoke sensing module along with the reference. Within the averaged particle size range of 0.4 μm to 1.4 μm , the smoke sensing module shows a $\pm 0.1\text{-}\mu\text{m}$ accuracy with respect to the laser-based reference.

Figure 3-17 shows the real-time mass concentration (PM4) reading comparison of the smoke sensing module and the reference (y-axis MC 4p0 = Mass Concentration PM4). From the 2000 $\mu\text{g}/\text{m}^3$ to 30000 $\mu\text{g}/\text{m}^3$

measurement range, the smoke sensing module can achieve $\pm 30\%$ relative measurement accuracy with respect to the reference. Some of this error can be attributed to the difference in placement of the smoke-sensing module and the reference in a chamber that is not exactly uniform. It is estimated that the real error level achievable is approximately $\pm 20\%$. Note that the lower bound measurement error is mainly limited to the quantization noise of the system. Enabling a higher signal chain gain, this limitation can be reduced.

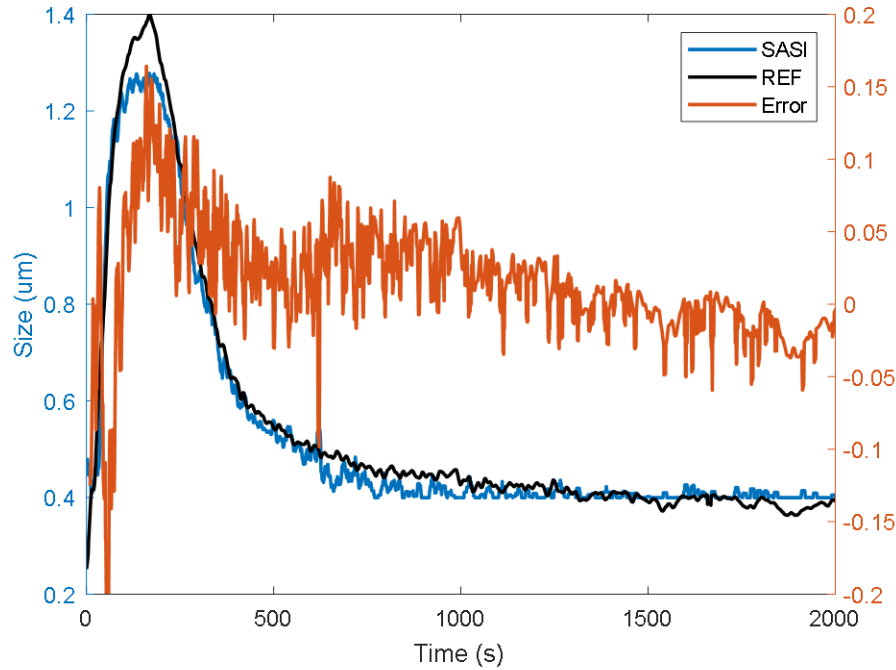


Figure 3-16. Real-Time Averaged Particle Size Measurement Comparison

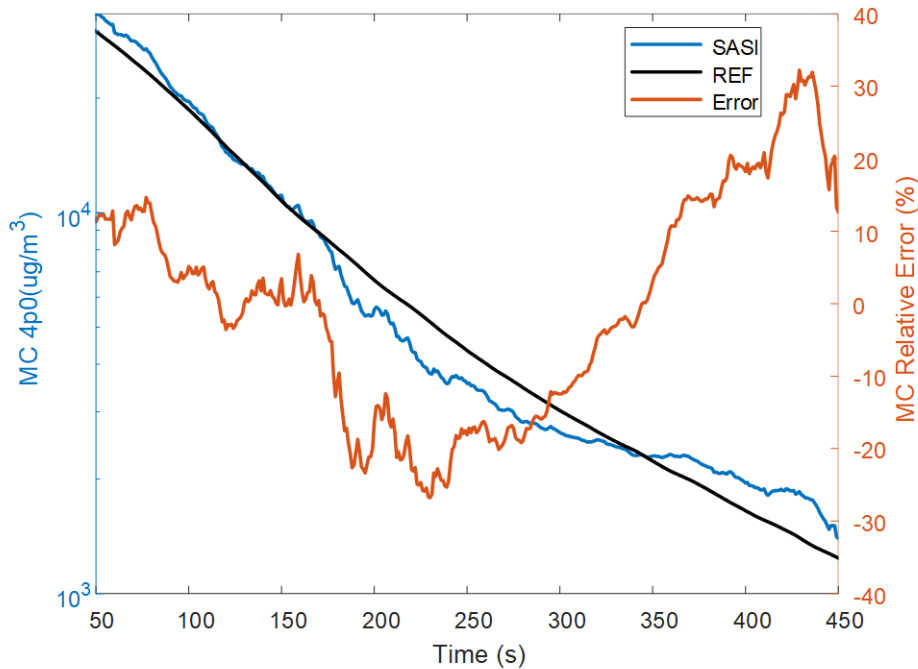


Figure 3-17. Real-Time Mass Concentration Measurement Comparison

3.4.4 Power Testing Results

The total system power is measured with a 9-V input supply. Table 3-3 summarizes the total current consumption for the 9-V battery. For typical low-power mode operation (number of pulses = 16; sampling time = 10 s), the average current is measured to be 5.8 μA as shown in Figure 3-18. This demonstrates the 10-year battery life capability using a standard 9-V alkaline battery typically used in smoke alarms. Figure 3-19 shows the average current consumption for the high-power mode which is entered when smoke is first detected and the early-warning threshold TH_0 is exceeded.

Note that the power is measured without UART communication enabled. Current consumption results in other configurations are also provided in Table 3-3.

Table 3-3. System Current Consumption for 9-V Battery With Different Configurations

NUMBER OF PULSES	SAMPLE TIME	CURRENT (μA)
16	10	5.8
16	1	17.4
128	1	75.7
300	1	127

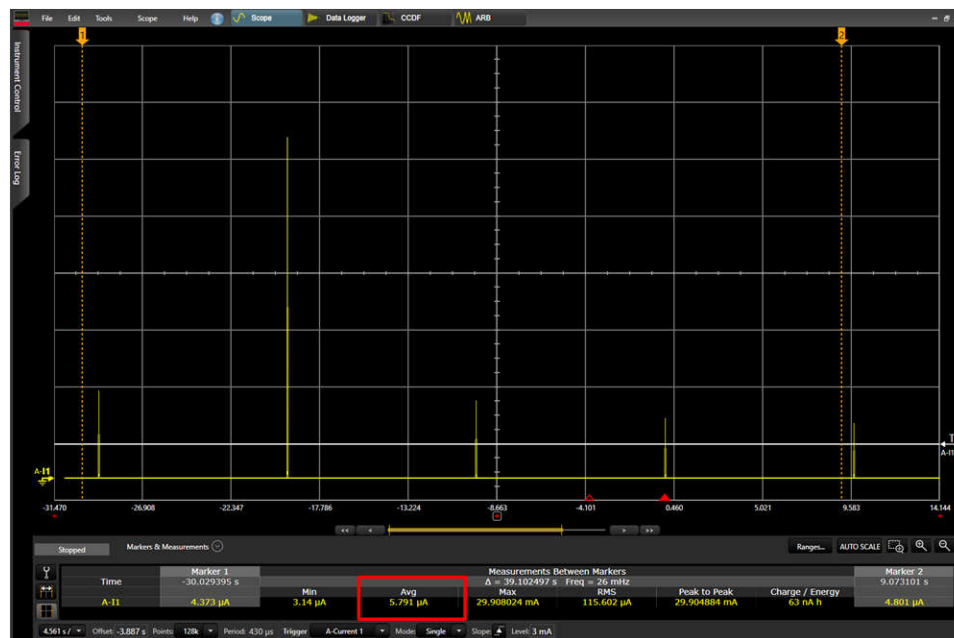


Figure 3-18. Transient Current Waveform of SASI Smoke Detection Module for Low-Power Mode (Number of Pulses = 16, Sample Period = 10 s)

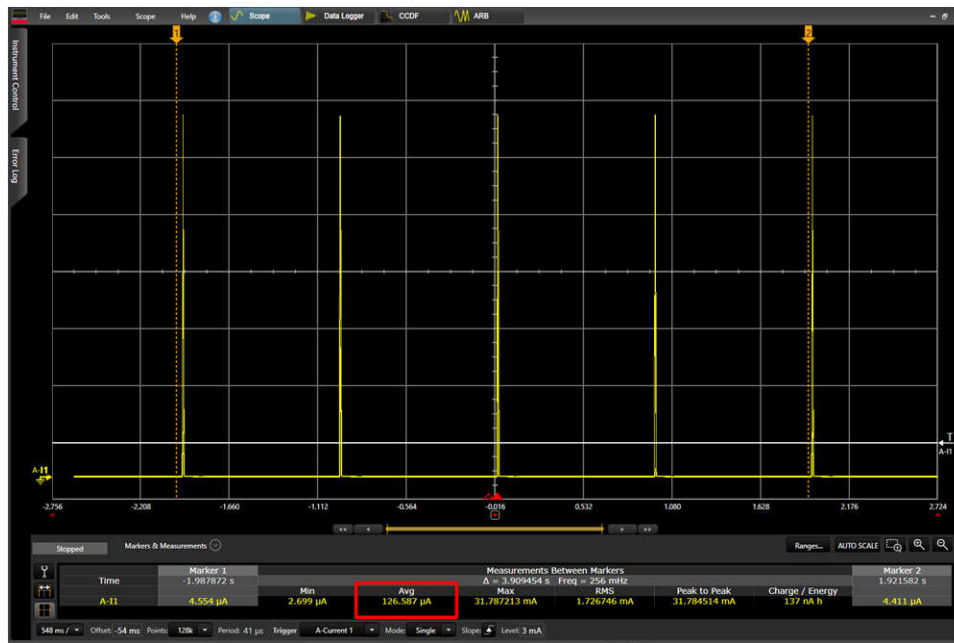


Figure 3-19. Transient Current Waveform of SASI Smoke Detection Module for High-Power Mode (Number of Pulses = 300, Sampling Period = 1 s)

3.4.5 Fire Room Smoke Testing

This section shows the plots of the transient recordings from the UL Fire Room tests for both the SASI smoke detection module and the optical obscuration reference meter. These plots demonstrate the successful smoke detection against various smoke types as well as the no false alarm result from the cooking nuisance source.

The raw response from the Blue and IR LED measurements are presented as a current transfer ratio (CTR). This measurement is the received photodiode current divided by the corresponding LED current. The ratio of the Blue and IR responses is also plotted to illustrate the usefulness to help distinguish various fire types. The reference measurement for the smoke data is captured by the reference meter and is given in units of obscuration rate (% / foot).

Figure 3-20 shows the transient plot of the *Go-No-Go Flaming Polyurethane* test, which includes both the Cooking Nuisance source (beginning of test up to 1.5 %/ft obscuration) and the *Flaming Polyurethane* source (ignited as the cooking nuisance source is turned off at the 1.5%/ft time). Figure 3-21 shows the transient plot for the *Wood Fire* test. Figure 3-22 shows the transient plot for the *Paper Fire* test. Figure 3-23 shows the transient plot for the *Smoldering Smoke* test. Figure 3-24 shows the transient plot for the *Smoldering Polyurethane* test.

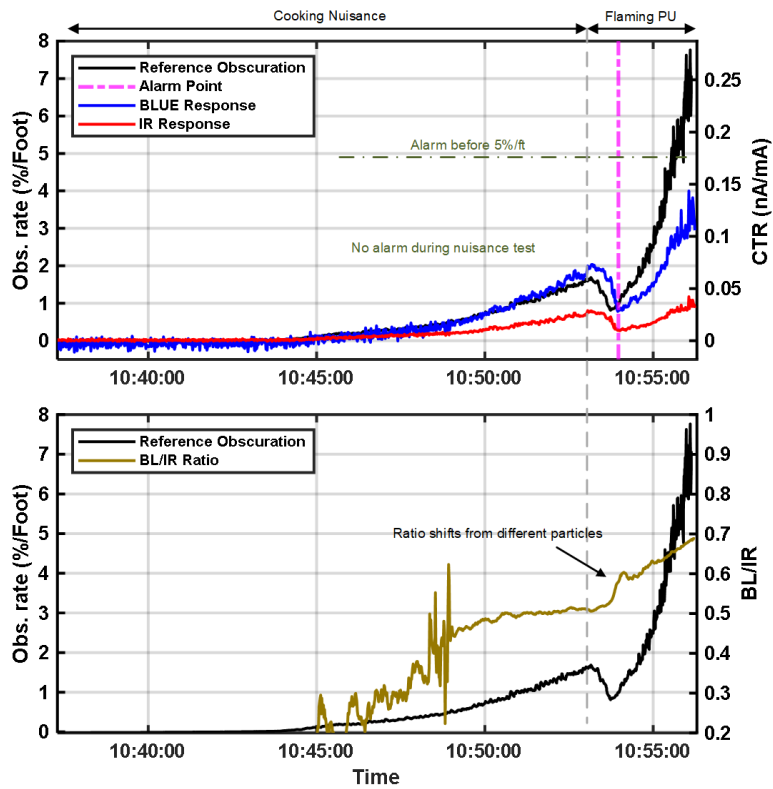


Figure 3-20. Transient Waveform of SASI Module at North Ceiling Location, Go-No-Go Nuisance With Flaming Polyurethane Foam Test (UL217 9th ed. Test 54)

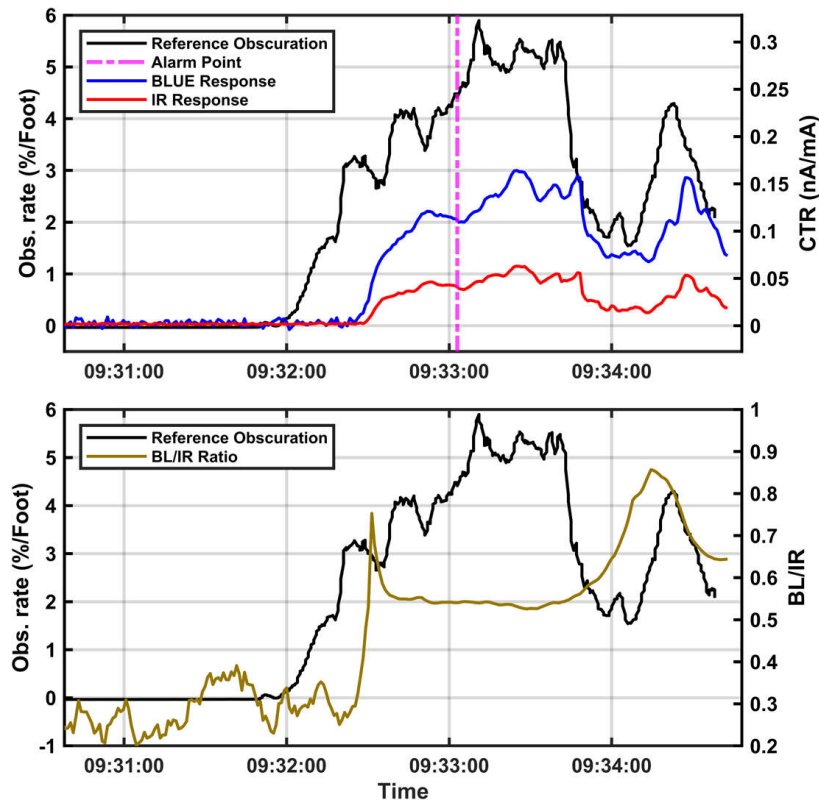


Figure 3-21. Transient Waveform of SASI Module at North Ceiling Location, Wood Fire Test (UL217 9th ed. Test 50.3)

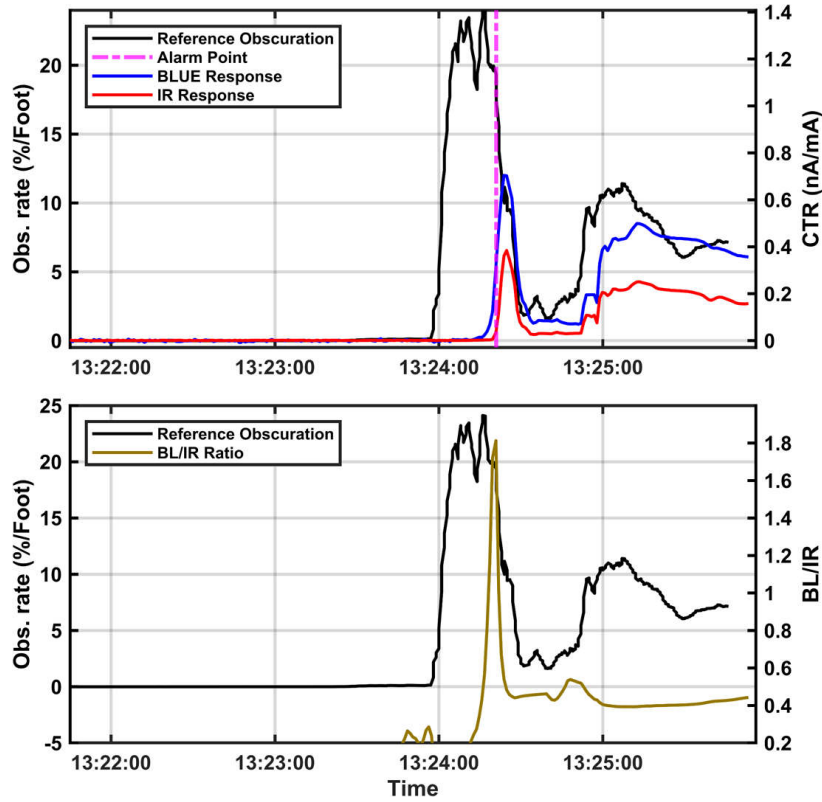


Figure 3-22. Transient Waveform of SASI Module at North Ceiling Location, Paper Fire Test (UL217 9th ed. Test 50.2)

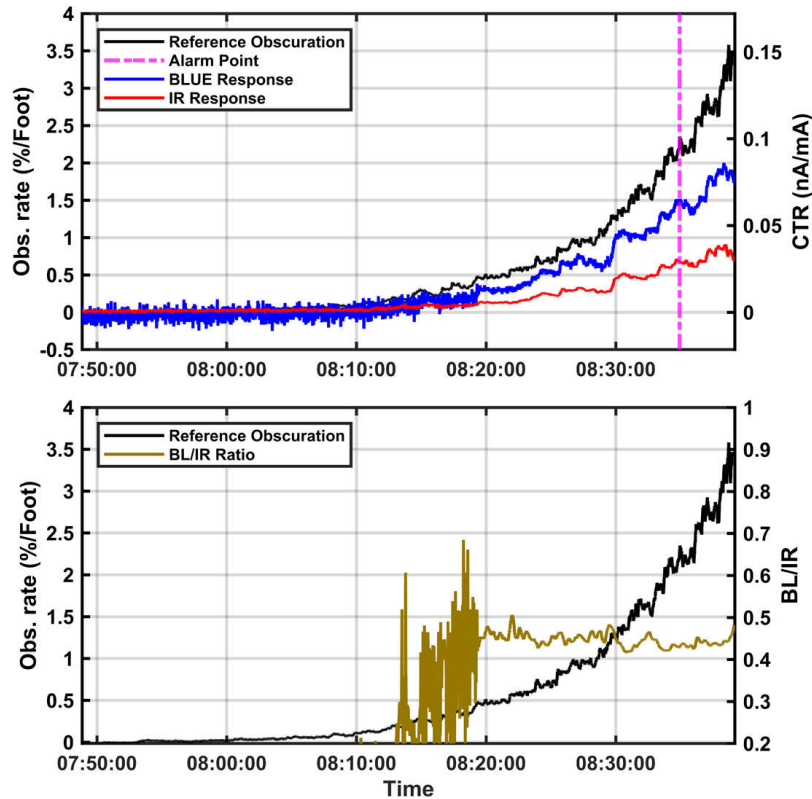


Figure 3-23. Transient Waveform of SASI Module at North Ceiling Location, Smoldering Smoke Test (UL217 9th ed., Test 51)

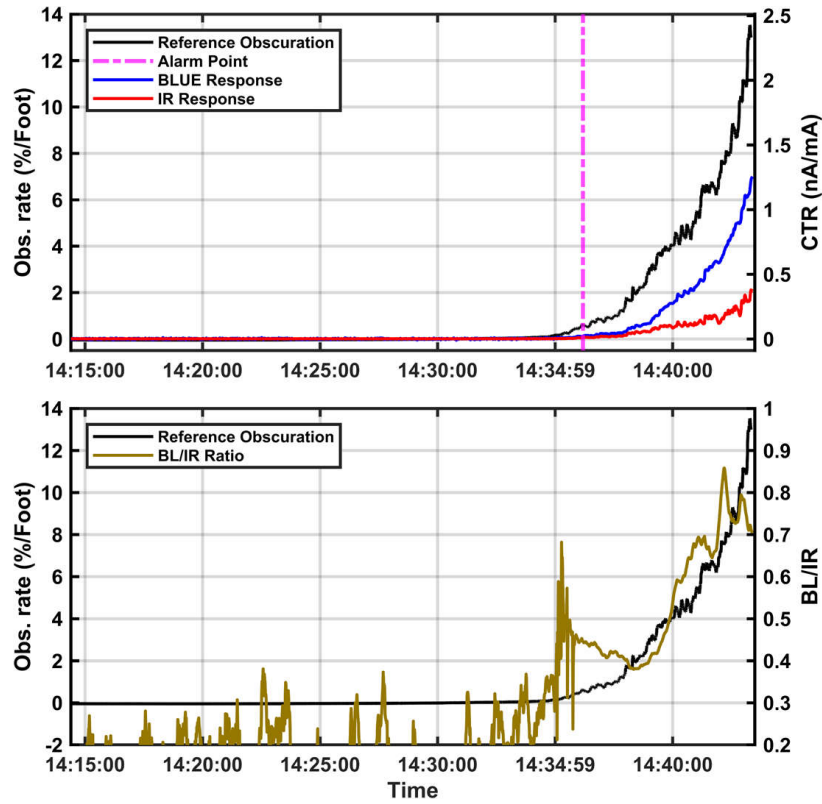


Figure 3-24. Transient Waveform of SASI Module at North Ceiling Location, Smoldering Polyurethane Foam Test (UL217 9th ed., Test 52)

4 Design and Documentation Support

4.1 Design Files

4.1.1 Schematics

To download the schematics, see the design files at [TIDA-010941](#).

4.1.2 BOM

To download the bill of materials (BOM), see the design files at [TIDA-010941](#).

4.1.3 CAD Files

To download the 3D print files for the optical assemblies, see the design files at [TIDA-010941](#).

4.2 Tools and Software

Tools

TINA-TI™ software Provides all the conventional DC, transient and frequency domain analysis of SPICE and much more. TINA has extensive post-processing capability allowing output of the results in the desired format. Virtual instruments allow selection of input waveforms and probe circuit nodes voltages and waveforms. The schematic capture of TINA-TI™ is truly intuitive - a real *quick start*.

Software

MSPM0 SDK Provides the ultimate collection of software, tools, and documentation to accelerate the development of applications for the MSPM0 MCU platform. The software is designed for peak performance and memory utilization, providing a consistent and cohesive experience with a wide variety of drivers, libraries, and easy-to-use examples under a single software package.

TIDA-010941 GUI A graphical user interface (GUI) was developed with Python for this reference design. Developers can log data, view particle information, and see whether smoke was detected. The GUI also streams the measurements to the terminal, printing both time and signal responses.

4.3 Documentation Support

1. Texas Instruments, [MSPM0L130x Mixed-Signal Microcontrollers](#) data sheet
2. Texas Instruments, [TLV906xS 10-MHz, RRIO, CMOS Operational Amplifiers for Cost-Sensitive Systems](#) data sheet
3. Texas Instruments, [TPS7A24 200-mA, 18-V, Ultra-Low I_Q, Low-Dropout Voltage Regulator](#) data sheet
4. Texas Instruments, [TS5A623157 DUAL 10-Ω SPDT ANALOG SWITCH WITH UNDERSHOOT/OVERSHOOT VOLTAGE PROTECTION](#) data sheet
5. Texas Instruments, [SN74LVC1G66 Single Bilateral Analog Switch](#) data sheet
6. Texas Instruments, [HDC2010 Low-Power Humidity and Temperature Digital Sensors](#) data sheet
7. Texas Instruments, [MSPM0L1306 LaunchPad™ development kit for 32-MHz Arm® Cortex®-M0+ MCU](#) tool folder
8. Texas Instruments, [MSPM0L1306 LaunchPad Development Kit \(LP-MSPM0L1306\)](#) user's guide
9. Texas Instruments, [MSPM0 software development kit \(SDK\)](#) tool folder
10. Texas Instruments, [MSPM0 SDK](#) TI developer zone
11. Texas Instruments, [Code Composer Studio Theia](#) user's guide
12. Texas Instruments, [MSPM0 SDK QuickStart Guide for CCS](#) user's guide
13. Texas Instruments, [MSPM0 SDK QuickStart Guide for CCS Theia](#) user's guide

4.4 Support Resources

TI E2E™ support forums are an engineer's go-to source for fast, verified answers and design help — straight from the experts. Search existing answers or ask your own question to get the quick design help you need.

Linked content is provided "AS IS" by the respective contributors. They do not constitute TI specifications and do not necessarily reflect TI's views; see TI's [Terms of Use](#).

4.5 Trademarks

TI E2E™, LaunchPad™, Code Composer Studio™, TINA-TI™, and are trademarks of Texas Instruments. Arm® and Cortex® are registered trademarks of Arm Limited. Python® is a registered trademark of Python Software Foundation. All trademarks are the property of their respective owners.

5 About the Author

BOYU SHEN is a Design Engineer with Kilby Labs, Texas Instruments focusing on circuit and system design for sensing applications. Boyu received the B.S. degree in electronic science and technology from the University of Science and Technology of China, Hefei, China, in 2015, and the Ph.D. degree in electrical and computer engineering from Oregon State University, Corvallis, OR, USA, in 2020.

THOMAS TSAI is a system engineer and manager at Kilby Labs, Texas Instruments, where he is responsible for the development of various sensing applications for Internet of Things. His expertise spans across signal processing, power control, RF, wireless communication and mixed signal system modeling. Thomas received his B.S. and Ph.D. degrees in electrical engineering from The Ohio State University, Columbus OH in 2007 and 2013, respectively. He has authored and coauthored 6 IEEE conference and journal papers and holds 16 patents.

DAVID STOUT is a systems designer at Texas Instruments, where he is responsible for developing reference designs in the industrial segment. David has over 18 years of experience designing Analog, Mixed-Signal, and RF ICs with more than 14 years focused on products for the industrial semiconductor market, in addition to nearly 8 years of experience designing system and circuit level designs for Fire Safety systems. David earned his bachelor of science in electrical engineering (BSEE) degree from Louisiana State University, Baton Rouge, Louisiana and a master of science in electrical engineering (MSEE) degree from the University of Texas at Dallas, Richardson, Texas.

URICA WANG is a software engineer at Texas Instruments, focusing on developing low level drivers and writing software for graphical code generation tools and fixed-function microcontrollers. Urica has 3 years of experience as an embedded software engineer and received her B.S. in Computer Engineering from Georgia Institute of Technology in 2020.

IMPORTANT NOTICE AND DISCLAIMER

TI PROVIDES TECHNICAL AND RELIABILITY DATA (INCLUDING DATA SHEETS), DESIGN RESOURCES (INCLUDING REFERENCE DESIGNS), APPLICATION OR OTHER DESIGN ADVICE, WEB TOOLS, SAFETY INFORMATION, AND OTHER RESOURCES "AS IS" AND WITH ALL FAULTS, AND DISCLAIMS ALL WARRANTIES, EXPRESS AND IMPLIED, INCLUDING WITHOUT LIMITATION ANY IMPLIED WARRANTIES OF MERCHANTABILITY, FITNESS FOR A PARTICULAR PURPOSE OR NON-INFRINGEMENT OF THIRD PARTY INTELLECTUAL PROPERTY RIGHTS.

These resources are intended for skilled developers designing with TI products. You are solely responsible for (1) selecting the appropriate TI products for your application, (2) designing, validating and testing your application, and (3) ensuring your application meets applicable standards, and any other safety, security, regulatory or other requirements.

These resources are subject to change without notice. TI grants you permission to use these resources only for development of an application that uses the TI products described in the resource. Other reproduction and display of these resources is prohibited. No license is granted to any other TI intellectual property right or to any third party intellectual property right. TI disclaims responsibility for, and you will fully indemnify TI and its representatives against, any claims, damages, costs, losses, and liabilities arising out of your use of these resources.

TI's products are provided subject to [TI's Terms of Sale](#) or other applicable terms available either on [ti.com](https://www.ti.com) or provided in conjunction with such TI products. TI's provision of these resources does not expand or otherwise alter TI's applicable warranties or warranty disclaimers for TI products.

TI objects to and rejects any additional or different terms you may have proposed.

Mailing Address: Texas Instruments, Post Office Box 655303, Dallas, Texas 75265
Copyright © 2023, Texas Instruments Incorporated